



LUND UNIVERSITY

Radiation dose to patients in diagnostic nuclear medicine. Implementation of improved anatomical and biokinetic models for assessment of organ absorbed dose and effective dose.

Andersson, Martin

2017

Document Version:

Publisher's PDF, also known as Version of record

[Link to publication](#)

Citation for published version (APA):

Andersson, M. (2017). *Radiation dose to patients in diagnostic nuclear medicine. Implementation of improved anatomical and biokinetic models for assessment of organ absorbed dose and effective dose.* [Doctoral Thesis (compilation), Medical Radiation Physics, Malmö]. Lund University: Faculty of Medicine.

Total number of authors:

1

General rights

Unless other specific re-use rights are stated the following general rights apply:

Copyright and moral rights for the publications made accessible in the public portal are retained by the authors and/or other copyright owners and it is a condition of accessing publications that users recognise and abide by the legal requirements associated with these rights.

- Users may download and print one copy of any publication from the public portal for the purpose of private study or research.
- You may not further distribute the material or use it for any profit-making activity or commercial gain
- You may freely distribute the URL identifying the publication in the public portal

Read more about Creative commons licenses: <https://creativecommons.org/licenses/>

Take down policy

If you believe that this document breaches copyright please contact us providing details, and we will remove access to the work immediately and investigate your claim.

LUND UNIVERSITY

PO Box 117
221 00 Lund
+46 46-222 00 00

Radiation dose to patients in diagnostic nuclear medicine

Implementation of improved anatomical and biokinetic models for assessment of organ absorbed dose and effective dose

MARTIN ANDERSSON

FACULTY OF MEDICINE | LUND UNIVERSITY 2017



Radiation dose to patients in diagnostic nuclear medicine

Implementation of improved anatomical and
biokinetic models for assessment of organ
absorbed dose and effective dose

Martin Andersson



LUND
UNIVERSITY

DOCTORAL DISSERTATION

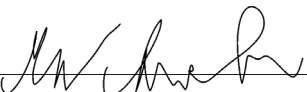
by due permission of the Faculty of Medicine, Lund University, Sweden.
To be defended at room 2005-7, DC, SUS, Malmö, 2017-04-21, 9:15

Faculty opponent

Professor John Harrison,
Oxford Brookes University and Public Health England, Chilton, Didcot, UK

Organization LUND UNIVERSITY	Document name DOCTORAL DISSERTATION	
	Date of issue 2017-04-21	
Author(s) Martin Andersson	Sponsoring organization	
Title and subtitle: Radiation dose to patients in diagnostic nuclear medicine - Implementation of improved anatomical and biokinetic models for assessment of organ absorbed dose and effective dose		
<p>Abstract</p> <p>Radiation absorbed dose estimations for patients undergoing diagnostic examinations in nuclear medicine are performed via calculations, based on models of the human body and on the radiopharmaceutical behaviour in the body. An adult mathematical model was created and the corresponding so called specific absorbed fractions (SAF) values were published by Snyder <i>et al.</i> (1974) which later were updated in Medical Internal Radiation Dose (MIRD) pamphlet 5 revised and pamphlet 11 (Snyder <i>et al.</i>, 1974; 1978).</p> <p>Mathematical models for a whole family of phantoms were created by Cristy and Eckerman (1987). To estimate the radiation risk to a population examined with a specific radiopharmaceutical, the effective dose is often calculated using the tissue weighting factors from ICRP Publication 60. This thesis focuses on revising absorbed dose calculations by using updated SAF values, which are based on mathematical models described by CT or MR images generated on real patients. These have later been modified to represent the reference person given in ICRP Publication 89. Together with the adoption of the new mathematical models, the updated definition of effective dose (ICRP, 2007) has been implemented.</p> <p>In Paper I an internal dosimetry computer program called "Internal Dose Assessed by Computer" (IDAC2.0) is presented and in Paper IV this software is used to calculate revised organ doses and the effective doses for five clinically important PET radiopharmaceuticals. Paper II presents a graphical user interface computer program created to facilitate arbitrary Monte Carlo simulations directly on the mathematical models for specific situations where predefined SAF values have to be applied, e.g. effective dose estimations from local skin contaminations. The specific absorbed fractions and the mathematical models are defined for predetermined structures which may be more or less realistic assumptions. In Paper III, new SAF values have been generated for the urinary bladder wall at different bladder volumes, allowing absorbed dose calculations for a dynamic urinary bladder, where the SAF value is dependent on the degree of urinary bladder filling.</p> <p>In order to calculate the absorbed dose, a biokinetic model is needed. A biokinetic model describes the transfer and distribution of the modelled radiopharmaceutical in different organs and tissues. Paper VI proposes a new biokinetic model for the element indium in ionic form and the absorbed doses and the effective dose are calculated for indium-111 and indium-113m ions.</p> <p>In nuclear medicine, procedures can be optimised on different parameters like diagnostic information, organ absorbed doses, or effective dose. Paper V is a review on dose management for conventional nuclear medicine imaging and PET, where the importance of several relevant parameters is discussed. The goal of the review paper is to highlight the need for establishing image quality criteria in nuclear medicine to the same extent as is done in X-ray imaging. This will facilitate observer performance studies which are needed in the search for optimal imaging conditions. The main contribution towards optimisation has up to now been the recommendation to adjust the administered activity by the patients weight. The dose management in nuclear medicine imaging requires more attention and there is a need for better use of new technology for individual patient dose management and for education and training.</p> <p>In conclusion, the work behind this thesis has aimed to develop and adopt more detailed and complex anatomical and biokinetic models to enable more realistic absorbed dose calculations for examinations with radiopharmaceuticals.</p>		
Key words: Diagnostic nuclear medicine, biokinetic models, internal dosimetry, absorbed dose, effective dose		
Classification system and/or index terms (if any)		
Supplementary bibliographical information	Language: English	
ISSN and key title	ISBN 978-91-7619-437-9	
Recipient's notes	Number of pages 62	Price
	Security classification	

I, the undersigned, being the copyright owner of the abstract of the above-mentioned dissertation, hereby grant to all reference sources permission to publish and disseminate the abstract of the above-mentioned dissertation.

Signature  Date 2017-03-16

Radiation dose to patients in diagnostic nuclear medicine

Implementation of improved anatomical and
biokinetic models for assessment of organ
absorbed dose and effective dose

Martin Andersson



LUND
UNIVERSITY

A doctoral thesis at a university in Sweden takes either the form of a single, cohesive research study (monograph) or a summary of research papers (compilation thesis), which the doctoral student has written alone or together with one or several other author(s).

In the latter case the thesis consists of two parts. An introductory text puts the research work into context and summarises the main points of the papers. Then, the research publications themselves are reproduced, together with a description of the individual contributions of the authors. The research papers may either have been already published or are manuscripts at various stages (in press, submitted, or in draft).

Cover illustration front: by Martin Andersson, a mesh version of the ICRP/ICRU adult reference computational phantoms.

Cover illustration back: by Mikael Gunnarsson, photograph of the author March 2017.

© Martin Andersson 2017

Lund University, Faculty of Medicine Doctoral Dissertation Series 2017:57

Department of Translational Medicine
Medical Radiation Physics Malmö
Skåne University Hospital
SE-205 02 Malmö, Sweden

ISBN 978-91-7619-437-9
ISSN 1652-8220

Printed in Sweden by Media-Tryck, Lund University
Lund 2017



”Ett bra riff kan lösa många konflikter”

Stefan Kärnström, musiker

Content

Acknowledgements.....	8
List of figures.....	9
Abbreviations	10
Original papers.....	11
Other related publications by the author	12
Preliminary reports.....	13
Summary.....	15
Populärvetenskaplig sammanfattning.....	17
<i>Chapter 1</i> Introduction and aim.....	19
<i>Chapter 2</i> Biokinetic modelling.....	23
Estimation of the total number of disintegrations	25
Descriptive modelling.....	26
<i>Chapter 3</i> Internal dose calculations	35
Anatomical models	36
ICRP/ICRU adult reference phantoms.....	37
Specific absorbed fraction values.....	38
Absorbed dose calculations	39
Sources of uncertainty in internal dosimetry	44
Biological effects.....	45
Effective dose calculations.....	46
<i>Chapter 4</i> Summary of papers	49
<i>Chapter 5</i> Discussion and future outlook	53
<i>Chapter 6</i> Conclusions	55
Bibliography	57

Acknowledgements

My sincere appreciation and thankfulness goes to:

- My supervisors:
 - *Sigrid Leide Svegborn* for taken me in and helping me evolve as a grad student. You started as my teacher but ended up as my friend.
 - *Sören Mattsson* for your inspiration and sharing your vast knowledge and always being there for me. I have really learned a lot from you. I appreciate that you always see the best in people and I will always be grateful that you have shared your international contacts with me.
 - *Lennart Johansson* for your support and sharing your knowledge of expertise to me. Even if we are more than 1 000 km apart you have always just been an email away.
 - *David Minarik* for your input and contribution.
- My co-authors:
 - *Marie Sydoff*, my only real colleague, thanks for introducing me to the graduate program.
 - *Ünal Ören*, even if we were in different research groups you always held my back. I can't express how glad I am that I had you as my roomie.
 - *Mauritius Hiller* for a good collaboration and for always helping me feeling welcome in the US.
- To the research group Center for Radiation Protection Knowledge at Oak Ridge National Laboratory, especially to Rich Leggett and Keith Eckerman for always having time and sharing your vast knowledge with me.
- To all the past and current members of the ICRP task group 36 for your support and help and hopefully I will continue to contribute to the group.
- To my present and past colleagues at the Medical Radiation Physics Malmö, Lund University and Radiation Physics, Skåne University Hospital, Malmö:
 - *LEO, Jonas J, Christian B, Karl Ö, Mattias J, Therese GB, Marcus P, Hanna H, Maria C, Hannie P, Simon K, Lena T, Magnus D, Pontus T, Daniel F, Marcus S, Kurt S, Peder K, Gertie J, Pernilla P, Sven M, Jonas S, Sofie C, Elias D, Fredrik N, Carl S, Kai N, Peter W, Veronica NL, Sven B x2, Viveca F, Michael G, Lars H, Anja, Anders T et al.* for creating a pleasant work atmosphere.
- To all of you at the department of Medical Radiation Physics in Lund, for me it has only been 20 km and not the other way around.
- And finally I would like to thank Sven Richter and the Swedish Radiation Safety Authority for financing my research otherwise this could never have happened.

List of figures

1. Decay corrected relative retention of $^{111}\text{In}^{3+}$ in blood plasma as a function of time after injection. The circles represent time points in the Simonsen *et al.* (2009) study. The red and blue lines represent fits to the measured data using two mathematical functions as presented in **Paper VI**.
2. Retention of ^{111}In in the kidneys and red blood cells as functions of time after injection. The red markers represent the fraction (in %) of ^{111}In in kidneys and red blood cells in rats (\circ) and dogs ($*$, \square) after intravenous administration of $^{111}\text{InCl}_3$ (McIntyre *et al.*, 1974; Jönsson, 1991). The blue line represents the biokinetic model for ionic indium proposed in **Paper VI**.
3. A descriptive biokinetic model for indium ions presented in ICRP Publication 53 (ICRP, 1987).
4. To the left is the former standardised GI-tract model (ICRP, 1980) and to the right is the IDAC2.0 (**Paper I**) version of the HATM given in ICRP Publication 100.
5. A biokinetic model for indium ions where the substance is excreted through the urinary bladder contents (**Paper VI**).
6. The proposed biokinetic model for systemic indium presented in **Paper VI**.
7. To the left, the biokinetic model with transfer coefficients for ^{111}In . To the right, the cumulated activities for all separate compartments and the time dependent curve for “Liver 2” (Nr 3) (**Paper I**).
8. The ICRP/ICRU adult male (left) and female (right) reference voxel phantoms. For the right pair, all object identifier numbers (OID) are shown and for the left only a few selected OIDs are shown.
9. Monoenergetic SAF values at different energies for different volumes of the urinary bladder contents as a source region to the urinary bladder wall (**Paper III**).
10. The internal dose computer program developed in **Paper I**, where the absorbed and effective doses are calculated out of predefined SAF values (Zankl *et al.*, 2012). The program is here presented for ^{18}F -FDG.
11. A method to enable absorbed dose calculations for relevant target regions and effective dose estimations from an arbitrary source region (**Paper II**).
12. The absorbed dose to the urinary bladder wall from a 300 MBq administration of ^{18}F -fluoride calculated with different constant voiding intervals based on the data given in ICRP Publication 128 (2015) (**Paper V**).
13. Absorbed dose to the urinary bladder wall for 11 cases to the left and to the right is the urinary bladder volume, the activity in the contents and the dynamic SAF from 0 to 20 hours after an $^{99\text{m}}\text{Tc}$ -MAG3 examination. The red line is the hypothetic activity in the bladder without any voiding (**Paper III**).
14. The effective dose per MBq for twelve clinically relevant and frequently used radiopharmaceuticals (**Paper V**).

Abbreviations

$A(t)$	Activity at time t
\tilde{A}	Total number of disintegrations
AUC	Area under the curve
D	Mean absorbed dose
E	Effective dose
FDG	Fluorodeoxyglucose, 2-deoxy-2-fluoro-D-glucose
FET	Fluoroethyltyrosine
FLT	Deoxyfluorothymidine
HAT	Human alimentary tract
ICRP	International Commission on Radiological Protection
IDAC	Internal dose assessed by computer
IDACSTAR	Internal dose assessed by computer★
LLI	Lower large intestine
MAG3	Mercaptoacetyltriglycine
MIRD	Medical Internal Radiation Dose
MCNP	Monte Carlo N-particle
OID	Object identifier number
Phantoms	Mathematical models
SAF	Specific absorbed fraction
ULI	Upper large intestine
w_R	Radiation weighting factor
w_T	Tissue weighting factor

Original papers

This thesis is based on the following six publications, which will be referred to by their Roman numerals:

- I. **Internal radiation dosimetry computer program, IDAC 2.0, for estimation of patient doses from radiopharmaceuticals**
Martin Andersson, Lennart Johansson, David Minarik, Sören Mattsson and Sigrid Leide Svegborn.
Radiation Protection Dosimetry, 2012. 150(1), 119-23
- II. **IDACSTAR: a MCNP application to perform realistic dose estimations from internal or external contamination of radiopharmaceuticals**
Ünal Ören, Mauritius Hiller and Martin Andersson.
Radiation Protection Dosimetry, 2016, doi: 10.1093/rpd/ncw221
- III. **Improved estimates of the radiation absorbed dose to the urinary bladder wall**
Martin Andersson, David Minarik, Lennart Johansson, Sören Mattsson and Sigrid Leide Svegborn
Physics in Medicine and Biology, 2014. 59, 2137-2182
- IV. **Organ doses and effective dose for five PET radiopharmaceuticals**
Martin Andersson, Lennart Johansson, David Minarik, Sören Mattsson and Sigrid Leide Svegborn.
Radiation Protection Dosimetry, 2016. 169(1-4), 253-258
- V. **Dose management in conventional nuclear medicine imaging and PET**
Martin Andersson and Sören Mattsson
Clinical and Translational Imaging, 2016 4(1), 21-30
- VI. **A biokinetic model and absorbed doses for systemic indium**
Martin Andersson, Sören Mattsson, Lennart Johansson and Sigrid Leide Svegborn.
Submitted to Physics in Medicine and Biology

Published papers have been reproduced with kind permission from Oxford University Press (**Paper I, II, and IV**), © IOP Publishing (**Paper III**), and Springer (**Paper V**). All rights reserved.

Other related publications by the author

- **Effective dose to adult patients from 338 radiopharmaceuticals estimated using ICRP biokinetic data, ICRP/ICRU computational reference phantoms and ICRP 2007 tissue weighting factors**

Martin Andersson, Lennart Johansson, David Minarik, Sigrid Leide Svegborn and Sören Mattsson.

EJNMMI Phys, 2014. 1:9

- **Erratum to: Effective dose to adult patients from 338 radiopharmaceuticals estimated using ICRP biokinetic data, ICRP/ICRU computational reference phantoms and ICRP 2007 tissue weighting factors**

Martin Andersson.

EJNMMI Phys, 2015. 2:22

- **Use of wall-less ^{18}F -doped gelatin phantoms for improved volume delineation and quantification in PET/CT**

Marie Sydoff, Martin Andersson, Sören Mattsson and Sigrid Leide Svegborn
Physics in Medicine and Biology, 2014. 59, pp 1097-1107

- **A phantom for determination of calibration coefficients and minimum detectable activities using a dual-head gamma camera for internal contamination monitoring following radiation emergency situations**

Ünal Ören, Martin Andersson, Christopher Rääf and Sören Mattsson
Radiation Protection Dosimetry 2016. 169(1–4), 297–302

- **Technological advances in hybrid imaging and impact on dose**

Sören Mattsson, Martin Andersson and Marcus Söderberg

Radiation Protection Dosimetry 2014. 165(1–4), 410–415 (invited)

- **Rules of the thumb and practical hints for radiation protection in nuclear medicine**

Sören Mattsson, and Martin Andersson

In: *Radiation Protection in Nuclear Medicine*, Editors: Sören Mattsson, Christoph Hoeschen. Springer Verlag, Germany, Berlin-Heidelberg, 2013 pp 151-159

Preliminary reports

Oral presentations:

- An upgrade of the internal dosimetry computer program IDAC. Andersson, M., Johansson, L., Minarik, D., Mattsson, S., Leide Svegborn, S. In: Medical physics in the Baltic states 2012 (Ed. by D. Adlienė), Technologija, Kaunas, Lithuania, 2012, pp 120-123
- Optimal voiding times and initial bladder after an ^{18}F -FDG administration in nuclear medicine. Andersson, M., Johansson, L., Minarik, D., Mattsson, S., Leide Svegborn, S. Swerays, Uppsala 21-23 August 2013
- Absorbed dose to the urinary bladder wall for different radiopharmaceuticals using dynamic S-values. Andersson, M., Johansson, L., Minarik, D., Mattsson, S., Leide Svegborn, S. EANM, Lyon, France Abstract: Eur J Nucl Med Mol Imaging (2013) 40 (suppl 2):S161
- IDAC2.0 a new generation of internal dosimetric calculations for diagnostic examinations in nuclear medicine using the adult ICRP/ICRU reference computational voxel phantoms. Andersson, M., Johansson, L., Minarik, D., Mattsson, S., Leide Svegborn, S. EANM, Lyon, France Abstract: Eur J Nucl Med Mol Imaging (2013) 40 (suppl 2):S175
- Revised dose calculations for iodide I-123, I-124, I-125 and I-131 for diagnostic investigations in nuclear medicine. Andersson, M., Mattsson, S., Minarik, D., Leide Svegborn, S., Johansson, L. SNMMI, St. Louis USA Abstract: J Nucl Med. (2014) 55 (Supplement 1):419
- A new voxel based method to generate dose coefficients for the source region “other organs and tissues”. Andersson, M., Minarik, D., Johansson, L Mattsson, S., Leide Svegborn, S. EANM, Gothenburg Abstract: Eur J Nucl Med Mol Imaging (2014) 41 (suppl 2):S237
- Organ doses and effective dose for five PET radiopharmaceuticals. Andersson, M., Johansson, L., Mattsson, S., Minarik, D., Leide Svegborn, S., Optimisation in X-ray and Molecular Imaging 2015, Gothenburg 2015
- Is individual dose assessment and risk estimation in diagnostic imaging needed? - and possible? Almén, A., Andersson, M., Mattsson S. Radiation Protection Week, Oxford, UK, 19-23 September, 2016
- IDACSTAR -a standalone program to easily Monte Carlo estimate the effective dose from internal or external contamination. Andersson, M., Ören, U. National meeting on medical physics, Kolmården, 2016

- EPA (USA) cancer risk models as an alternative to effective dose to estimate the radiation risk for individual patients in health care. Andersson, M., Eckerman, K., Mattsson, S. National meeting on medical physics, Kolmården, 2016
- Creating Monte Carlo dose risk estimations based direct on CAD output files and validating the estimation using a 3D printer. Andersson, M., Herrnsdorf, L. National meeting on medical physics, Kolmården, 2016

Posters:

- Use of wall-less radionuclide doped gel phantoms to determine the influence of non-active phantom walls in ^{18}F PET/CT and ^{123}I SPECT/CT activity quantification and outlining of tissue volume. Sydoff, M., Andersson, M., Mattsson, S., Leide Svegborn, S. EANM, Lyon, France Abstract: Eur J Nucl Med Mol Imaging (2013) 40 (suppl 2):S304
- A study of the feasibility of using slabbing to reduce tomosynthesis review time Dustler, M., Andersson, M., Förnvik, D., Timberg, P., Tingberg, A. SPIE Medical Imaging, San Diego, CA, USA 2013 DOI:10.1117/12.20 06987 (also in reviewed proceedings)
- Sensitivity analysis of the absorbed dose to the dynamic urinary bladder wall. Andersson, M., Johansson, L., Minarik, D., Mattsson, S., Leide Svegborn, S. Radiobiology: Man-made radiation. Gomel, Belarus 2014
- Revised dose estimations for Tc-99m-pertechnetate for diagnostic nuclear medicine procedures in adults. Andersson, M., Johansson, L., Minarik, D., Mattsson, S., Leide Svegborn, S. EANM 2015, Hamburg, Germany
- A phantom for determination of calibration coefficients and minimum detectable activities using a SPECT/CT for internal contamination monitoring following radiation emergency situations. Ören, Ü., Andersson, M., Rääf, C.L., Mattsson, S. Optimisation in X-ray and Molecular Imaging 2015, Gothenburg 2015
- Improved radiation dosimetry for lung ventilation scintigraphy. Andersson, M., Johansson, L., Minarik, D., Mattsson, S., Leide Svegborn, S. World Molecular Imaging Congress 2015, 2-5th September 2015 Honolulu, Hawaii, USA
- New estimation of the effective dose for nuclear medicine examinations. Andersson, M., Johansson, L., Minarik, D., Mattsson, S., Leide Svegborn, S. Malmö Cancer Center, 2015 Ystad
- IDACSTAR -a standalone program to easy create Monte Carlo voxel simulated customized dose estimations. Ünal, Ö. Hiller, M., Andersson, M. SNMMI 11-15 June 2016 San Diego, CA, USA
- 3D-grapical representation of source geometries in lattice structures using the Monte Carlo Code MCNP. Andersson, M. Schwarz, R. & Hiller, M. Radiation Protection Week, 19-23 September, Oxford, 2016

Summary

Radiation absorbed dose estimations for patients undergoing diagnostic examinations in nuclear medicine are performed via calculations, based on models of the human body and on the radiopharmaceutical behaviour in the body. An adult mathematical model was created and the corresponding so called specific absorbed fractions (SAF) values were published by Snyder *et al.* (1974) which later were updated in Medical Internal Radiation Dose (MIRD) pamphlet 5 revised and pamphlet 11 (Snyder *et al.*, 1974; 1978). Mathematical models for a whole family of phantoms were created by Cristy and Eckerman (1987). To estimate the radiation risk to a population examined with a specific radiopharmaceutical, the effective dose is often calculated using the tissue weighting factors from ICRP Publication 60. This thesis focuses on revising absorbed dose calculations by using updated SAF values, which are based on mathematical models described by CT or MR images generated on real patients. These have later been modified to represent the reference person given in ICRP Publication 89. Together with the adoption of the new mathematical models, the updated definition of effective dose (ICRP, 2007) has been implemented.

In **Paper I** an internal dosimetry computer program called “Internal Dose Assessed by Computer” (IDAC2.0) is presented and in **Paper IV** this software is used to calculate revised organ doses and the effective doses for five clinically important PET radiopharmaceuticals. **Paper II** presents a graphical user interface computer program created to facilitate arbitrary Monte Carlo simulations directly on the mathematical models for specific situations where predefined SAF values have to be applied, *e.g.* effective dose estimations from local skin contaminations. The specific absorbed fractions and the mathematical models are defined for predetermined structures which may be more or less realistic assumptions. In **Paper III**, new SAF values have been generated for the urinary bladder wall at different bladder volumes, allowing absorbed dose calculations for a dynamic urinary bladder, where the SAF value is dependent on the degree of urinary bladder filling.

In order to calculate the absorbed dose, a biokinetic model is needed. A biokinetic model describes the transfer and distribution of the modelled radiopharmaceutical in different organs and tissues. **Paper VI** proposes a new biokinetic model for the element indium in ionic form and the absorbed doses and the effective dose are calculated for indium-111 and indium-113m ions.

In nuclear medicine, procedures can be optimised on different parameters like diagnostic information, organ absorbed doses, or effective dose. **Paper V** is a review on dose management for conventional nuclear medicine imaging and PET, where the importance of several relevant parameters is discussed. The goal of the review paper is to highlight the need for establishing image quality criteria in nuclear medicine to the same extent as is done in X-ray imaging. This will facilitate observer performance studies which are needed in the search for optimal imaging conditions. The main contribution towards optimisation has

up to now been the recommendation to adjust the administered activity by the patients weight. The dose management in nuclear medicine imaging requires more attention and there is a need for better use of new technology for individual patient dose management and for education and training.

In conclusion, the work behind this thesis has aimed to develop and adopt more detailed and complex anatomical and biokinetic models to enable more realistic absorbed dose calculations for examinations with radiopharmaceuticals.

Populärvetenskaplig sammanfattning

Diagnostiska undersökningar inom nuklearmedicin används för att påvisa sjukdomstillstånd genom att studera fysiologiska, metabola och kemiska processer i kroppen. Metoden går ut på att koppla ett radioaktivt ämne till en bärarsubstans vilken styr var upptaget kommer att ske. En vanlig metod för att avbilda tumörer är exempelvis att använda socker som bärarsubstans av ett radioaktivt ämne. Det märkta sockret söker sig bland annat till tumören, som har en större energiförbrukning än resten av kroppen. På så sätt kan tumören avbildas genom att detektera sönderfallet av det radioaktiva ämnet.

Fördelen med att använda sig av strålningsdiagnostik är att den medger mätning utanför kroppen och är en relativt enkel undersökning. En nackdel är att strålningen som används är joniserande och har en biologisk påverkan på kroppen. Inom diagnostisk nuklearmedicin administreras små mängder av ett spårämne, av strålslag som ger relativt liten biologisk påverkan, vilket medför att det inte blir några akuta strålskador. Intresset fokuseras istället på den eventuellt förhöjda risken att lång tid efter undersökningen få en strålningsinducerad cancer. Den ökade strålningsinducerade cancer risken är liten i förhållande till den normala cancerförekomsten i en population och därför baseras beräkningarna till en referenspopulation som främst bygger på erfarenheter från atombombsöverlevande från Nagasaki och Hiroshima.

För att kunna utföra riskuppskattningar baseras beräkningarna på två modeller; en biologisk samt en matematisk. Den biologiska modellen försöker uppskatta hur det radioaktiva läkemedlet fördelar sig i kroppen och därmed var i kroppen sönderfallen sker. När alla sönderfall som sker i kroppen har blivit lokaliserade med hjälp av en generell populationsmodell appliceras dessa sönderfall på en matematisk modell. Den matematiska modellen uppskattar var och hur stor energideponeringen är från varje sönderfall. Genom att göra dessa två uppskattningar kan en absorberad dos beräknas för olika strålkänsliga organ och sedan användas som en indikator för att uppskatta en biologisk effekt.

I denna avhandling har en ny biologisk modell skapats för grundämnet indium i jonform (In^{3+}), vilken beskriver indiums fördelning i kroppen mer realistiskt än tidigare modeller. De andra arbetena handlar om att förbättra den matematiska modellen för stråldosberäkningarna. Tidigare har det matematiska fantomet varit baserat på linjära och kvadratiske ekvationer, likt godistillverkaren Bassetts[®] maskot Bertie. Det fantomet har nu ersatts med mer detaljerade modeller baserade på CT- och MR-bilder från verkliga personer.

Samtidigt med införandet av mer realistiska matematiska modeller har också en uppdaterad version av riskkoefficienterna för olika strålkänsliga organ använts. Man utgår fortfarande från de överlevande i Hiroshima och Nagasaki, men risken baseras nu på risken att insjukna i cancer istället för på risken att dö i cancer.

Målet med avhandlingen är att skapa mer detaljerade modeller för hur de radioaktiva ämnena omsätts i kroppen, hur de bestrålar olika organ och vilken risk detta kan innebära.

Chapter 1

Introduction and aim

Diagnostic nuclear medicine, more recently also named functional molecular imaging, deals with medical procedures performed to help diagnose a variety of diseases. The procedures are based on the use of small (or tracer) amounts of radioactive material, where a radionuclide is attached to a ligand with specific affinity to a physiological, metabolic, or receptor-specific process. Unlike other imaging systems, which show anatomy and structure in detail, nuclear medicine can provide information on parameters like *e.g.* tissue blood flow, metabolism, and expression of cell receptors in normal and abnormal cells. The use of a radioactive tracer is extremely sensitive and tracer concentrations down to 10^{-12} mol/L can be measured. The method is also non-invasive and quite easy to use. However, to be able to detect a photon from a radioactive decay in the patient, a relatively high photon energy is required, which may create a biological effect within the body. The small risk to later in life develop a radiation-induced cancer from a diagnostic radiopharmaceutical is currently estimated based on the quantity effective dose (E). The effective dose is one of several parameters used to justify the clinical exposure with ionising radiation to diagnose pathologies in patients. The effective dose from a radiopharmaceutical depends on where the ionisation occurs and the total number of disintegrations and where they take place within the human body. To determine the total number of disintegrations a biokinetic model is created, where the radioactive substance is followed from injection until only an insignificant amount of the tracer remains in the body.

The purpose of a biokinetic model is to estimate the spatial and temporal distribution accounting for the decays associated with an examination using radiopharmaceuticals. A biokinetic model is created by determining which parts of the body that have an increased uptake of the radiopharmaceutical. The next step is to quantify these uptakes by means of available imaging devices, single detectors, or measurements of samples (like blood, urine, and faeces) during a time period after administration of the radiopharmaceutical. These data are then the base for information about time variation of activity in various organs. If enough data is gathered a complete system describing the transport of the tracer can be created. This method to account for transfer between organs is called compartmental modelling and is constructed mathematically by defining transfer rates of the radionuclide within different parts of the body. There are several parameters that determine the total number of disintegrations in the total body or the specific organs: the administered activity, the physical half-life of the radionuclide, the residence time of the substance, and its excretion rate via different pathways. If a biokinetic model can be constructed, there is a possibility to estimate the absorbed dose contribution from each disintegration. There are biokinetic models which are created from older studies using now outdated imaging devices

or like in the case of ionic indium only based on animal data. These biokinetic models should be subject for revision.

To be able to estimate the location of the tracer and how much energy is deposited inside the patient, the International Commission on Radiological Protection (ICRP) jointly with the International Commission on Radiation Units and Measurements (ICRU) have created models of reference persons resembling an adult male of 73 kg and a female of 60 kg. Mathematical models describing the energy deposition from a disintegration are also referred to as phantoms in this thesis. ICRP has created biokinetic models for a large number of radiopharmaceuticals (ICRP, 1979; 1987; 1998; 2008; 2015) and performed dose estimations. As of yet, the dose estimations from ICRP have been based on stylised mathematical models, which use linear and quadratic equation models of organ and tissue shapes. The mathematical models were first introduced in the Medical Internal Radiation Dose (MIRD) pamphlet 11 (Snyder *et al.*, 1975) improved, and completed with models representing other ages by Cristy and Eckerman (1987). Furthermore, dose calculations are generally performed using a fixed urinary bladder with a constant volume, independent on physiological or biological parameters. These simplifications may not result in a fully realistic representation of the body.

During the last decades, the ICRP has published several improvements of more detailed biokinetic and anatomical models. These improvements need to be implemented into the dose estimations of radiopharmaceuticals to be able to perform more realistic dose estimations. ICRP updated the basic anatomical and physiological data for the reference person in 2002 (ICRP, 1975; 2002) and therefore new mathematical models had to be created. Reference phantoms for adults based on CT and MR images from a real adult male and female, rather than mathematical models, were published in 2009 (ICRP, 2009). These phantoms resembled the predefined anatomical values regarding height and weight and the organs and tissues were adjusted according to the specifications given in the publication of anatomical reference values (ICRP, 2002). In 2007, ICRP published a new set of tissue weighting factors for calculation of the radiation protection unit effective dose, and several new organs and tissues were assigned weighting factors (ICRP, 1990; 2008). In the new reference phantoms, all the organs and tissues needed for the revised effective dose calculations were included and the phantoms were also created to be able to adopt a new human alimentary tract (HAT) model, describing the transfer of materials within this region (ICRP, 2006).

The overall aim of this thesis is to implement the ICRP/ICRU adult voxel phantoms for diagnostic nuclear medicine, enabling improved radiation dose estimations for diagnostic procedures with radiopharmaceuticals.

The specific aims of the thesis were to:

- create a new internal dosimetry computer program, which could perform absorbed dose calculations on the new voxel phantoms and estimate the effective dose based on the tissue weighting factors in ICRP Publication 103.
- modify existing biokinetic models for a number of radiopharmaceuticals, so that the models can be used by the recently created computer program.
- create a new biokinetic model for indium ions (In^{3+}) and perform dose calculations.
- estimate the absorbed dose to the urinary bladder wall for various degree of filling rate and volume of the bladder.
- enable a method to make Monte Carlo simulations with voxel phantoms, more user friendly.

Chapter 2

Biokinetic modelling

The main objective of biokinetic modelling in nuclear medicine is to create a model, which describes the distribution of the decays of the radionuclide. Such a model does not necessarily need to be physiologically and metabolically realistic. The model can be constructed in different ways, but all models are based on actual measured radionuclide data preferentially from healthy human volunteers. Patient data are generally measured from blood or urine samples, or may be quantified with SPECT/CT or PET/CT images. The radiopharmaceuticals can be administered via different routes depending on the examination, *e.g.* intravenously, orally, or via inhalation. Depending on the route of administration and the chemical properties of the radiopharmaceutical, the uptake in and excretion from various organs and tissues will differ. Therefore, it is important to measure the organ/tissue radionuclide content at different time points after administration. The uptake phase is often shorter than the retention phase and it is therefore important to make frequent measurements directly after the administration. To estimate the retention in various organs and tissues, measurements should continue until only an insignificant amount of the radionuclide remains in the body, which means that the physical decay of the tracer also has to be taken into account.

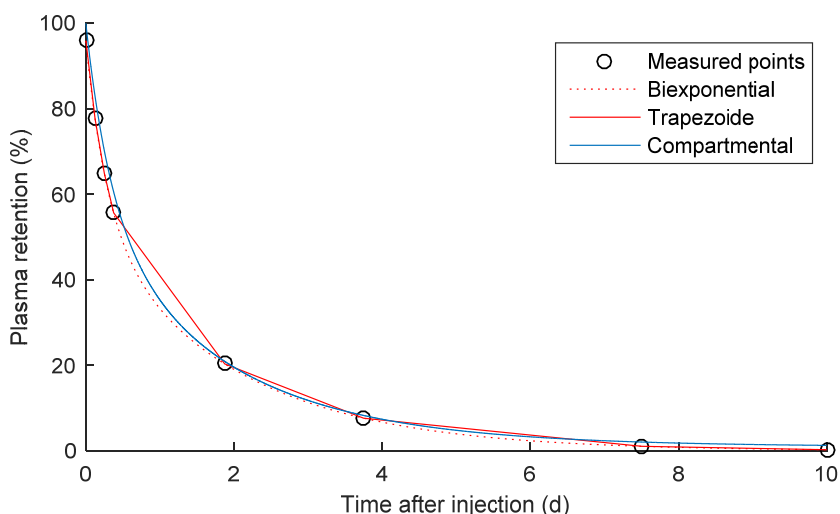


Figure 1.

Decay corrected relative retention of $^{111}\text{In}^{3+}$ in blood plasma as a function of time after injection. The circles represent time points in the Simonsen *et al.* (2009) study. The red and blue lines represent fits to the measured data using two mathematical functions as presented in **Paper VI**.

In Figure 1, decay corrected average plasma concentration of ionic indium from 15 healthy subjects are shown (Simonsen *et al.*, 2009). For intravenous administration, the indium concentration starts at 100 % and decreases as indium begins to distribute in the human body. To estimate the total number of disintegrations or the concentration at a specific time, a biokinetic model can be constructed. There are mainly three different methods to estimate the cumulated activity: numerical integration, least squares criterion, and compartmental modelling (Koepppe, 1996; Stabin, 2008). All are briefly described below.

All organs and tissues or other relevant structures which have an increased activity concentration in relation to the normal background uptake should be included as individual parts in the creation of the biokinetic model.

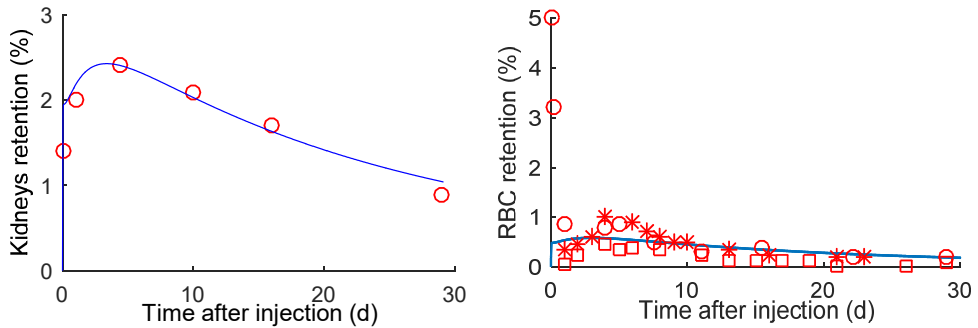


Figure 2. Retention of ^{111}In in the kidneys and red blood cells retention as functions of time after injection. The red markers represent the fraction (in %) of ^{111}In in kidneys and red blood cells in rats (○) and dogs (*, □) after intravenous administration of $^{111}\text{InCl}_3$ (McIntyre *et al.*, 1974; Jönsson, 1991). The blue line represent the biokinetic model for ionic indium proposed in **Paper VI**.

The aim of the ICRP biokinetic modelling (ICRP, 1987; 1998; 2008; 2015) is to create representative models for healthy individuals. The experimental biokinetic data, are on the other hand often based on patients. However, even for a dedicated tracer the uptake in the targeted organ is just a small fraction of the injected activity (*e.g.* 2-5 % for dedicated brain tracers) (ICRP, 2015). Thus, as only minor alterations of the uptake in other organs are expected, the overall biokinetic data is likely relevant also for healthy individuals. In some cases, there are not sufficient human data to create a biokinetic model and in these cases animal data could be used instead. However, a biokinetic model based too heavily on animal measurements is less likely to predict a realistic human model. If animal data is needed it is better to use data from mammals of the same size as humans, such as dogs and monkeys as opposed to rats and mice. Examples of an uptake and retention phase in the kidneys and red blood cells are shown in Figure 2 where data from dogs and rats are presented at different time points after injection of $^{111}\text{InCl}$ (McIntyre *et al.*, 1974; Jönsson, 1991).

Estimation of the total number of disintegrations

The cumulated activity, or total number of disintegrations, is estimated by integration of the activity as function of time in various organs or tissues. Examples of results of the most common estimation methods are presented in Figure 1. The trapezoid method is a type of numerical integration using the measured data directly. Using least squares estimation or compartmental modelling, a function is fit to the data which may then be integrated. A sum of exponential functions is often optimised by least square criteria and transfer coefficients in a compartmental model are often developed using a maximum likelihood method *e.g.* SAAM II (Barrett *et al.*, 1998). Both the trapezoid method and the method based on the sum of exponential functions are calculated for each organ and tissue independently, whereas compartmental modelling accounts for transfer of activity between relevant organs and tissues.

Numerical integration

The easiest method to calculate the total number of disintegrations \tilde{A} is to use the trapezoidal method:

$$\tilde{A} = \frac{\sum_i (f(t_i) + f(t_{i+1}))}{2} \Delta t_{i,i+1} \quad (2.1)$$

where $f(t_i)$ is the activity in the organ or tissue i and $\Delta t_{i,i+1}$ is the time difference between the two measurements $i, i + 1$. The trapezoid method will only be accurate with a constant linear retention. For a convex distribution it will underestimate the cumulated activity and opposite for a concave distribution. Furthermore, this method does not take remaining activity after the last measurements into account, which may cause a large underestimation of the total number of disintegrations if the radionuclide, or its radionuclide contaminants, has a long physical half-life.

Least squares criterion

The least squares criterion is based on minimising the sum of the squared distance from the estimated line to the measured points. The most common way is to assume that a sum of first order exponentials can be used to predict the model. In the example in Figure 1 a biexponential equation is used to estimate the area under the curve (AUC) and including a component for the physical decay reflects the total number of disintegrations. The biexponential equation is given by:

$$\frac{A(t)}{A(0)} = Ae^{-\lambda_{BioA}t} + Be^{-\lambda_{BioB}t} \quad (2.2)$$

where $A(t)$ is the time dependent activity at time t , λ_{BioA} and λ_{BioB} are the retention constants and A and B are constants with the criteria that $A + B = 1$. Unlike numerical

integration using the trapezoid method, integration of the biexponential function is not limited to the last measured point. The λ_{BioA} and λ_{BioB} constants may be connected to biological properties such as a fast and a slow, known or unknown process. Using the sum of first order exponentials to fit data points often results in a fit which is well optimised. There is no limit on how many terms to include in the sum of exponentials but the number included should reflect the accuracy of the data the summation is based on. Usually for modelling of radiopharmaceuticals transfer, there are no meaning more than two or three terms of exponentials.

Compartmental modelling

Compartmental modelling is a mathematical representation of the body or an area of the body created to study physiological or pharmacological kinetic characteristics. The transfer rate constants describe the probability of a tracer to be transferred from one compartment to another per unit time. Compartmental modelling combine all measured data points into one system. As an example, the amount of indium in plasma and red blood cells (Figure 1) or plasma retention and kidney uptake (Figure 2) may thus be connected. The concept of compartmental modelling is to create a system in which all tracers are placed in interconnected compartments. The probabilities of transfer between compartments are concentration and time independent (Goris, 2011). All compartments in a model belong to a pool, which often represents an organ or a tissue. In Figure 6 the liver pool is constructed out of two compartments. The compartments are connected with first order kinetics, meaning that transfer rates are constant and that the tracer flow only depends on the trace amount in a compartment (Giussani and Uusijärvi, 2011). This means that compartmental modelling does not account for saturation, as present for *e.g.* thyroid uptake of iodide, or that the tracer would affect the biological process.

Descriptive modelling

Descriptive modelling is a form of the modelling based on least squares criteria, and is the modelling type most frequently used by the ICRP for radiopharmaceuticals. The organs are often assumed to have an instantaneous uptake and the model only describes the excretion from that organ to the urine and faeces. It assumes immediate fractional uptake F_s in pool S and a sum of exponentials describes excretion and uptake according to:

$$\frac{A_S(t)}{A_0} = F_s \sum_{j=n+1}^{n+m} a_j \sum_{i=1}^n \left\{ a_i \frac{T_i}{T_i - T_j} \left[e^{\left(\frac{-\ln(2)}{T_{i,eff}}\right)t} - e^{\left(\frac{-\ln(2)}{T_{j,eff}}\right)t} \right] \right\} \quad (2.3)$$

where $A_S(t)/A_0$ is the fraction of injected activity at time t in pool S , a is the fraction of F_s uptake j or elimination i with the corresponding biological half-time T .

For most descriptive models presented in ICRP Publication 53, 80, 106, and 128, a special case of equation 2.3 is assumed, where an immediate uptake in the pool S is assumed:

$$\frac{A_S(t)}{A_0} = F_S \sum_{i=1}^n a_i e^{\left(\frac{-\ln(2)}{T_{i,eff}}\right)t} \quad (2.4)$$

Figure 3 shows a descriptive biokinetic model for ionic indium published in ICRP Publication 53 based on equation 2.4. The ICRP model of indium is created on animal studies of mice (Castronovo *et al.*, 1971; 1973), which assumed an initial uptake of 30 % in the red (active) bone marrow, 7 % in the kidneys, 20 % in the liver, 1 % in the spleen, and the remaining activity was given to a pool resembling a general background uptake often called “remainder” or “other soft tissue”. The initial model assumed no excretion of indium, but in ICRP Publication 53 an excretion component was included based on data from mice. This excretion was not connected to any specific biological process.

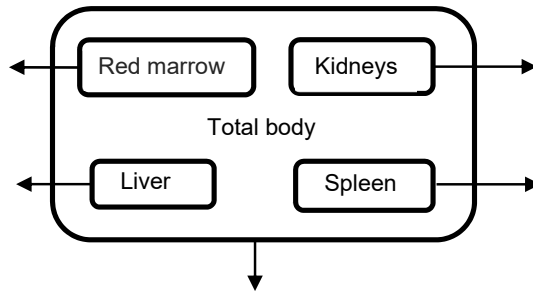


Figure 3. A descriptive biokinetic model for indium ions presented in ICRP Publication 53 (ICRP, 1987).

The most common method used in ICRP Publication 128 is to connect the excretion from the compartments to a real biological process, where the substance is transferred via the kidneys to the urinary bladder before leaving the body, or is passed through the gastrointestinal tract. The measurements of the activity in urine are often performed in biokinetic studies to be able to model a realistic urinary excretion. Measurement of activity in samples of faeces are also preferable, but faeces collection is often considered unpractical. The ICRP have defined standardised biokinetic models to help create more realistic compartmental models if there is a lack of data. But all models should strive to be based on real measurements if it is possible and to use ICRP standardised models when needed.

ICRP standardised models

When developing a compartment model, all radioactive substances need to be located within the body. Gathering data to construct a complete compartment model is not always possible and therefore ICRP has developed several standardised models (ICRP, 1980; 2006) to facilitate the development of realistic biokinetic models based on activity in samples of

various kinds, like blood, urine, or exhaled air. The ICRP has two different blood models: one for radiopharmaceuticals which have a very short physical half-life (seconds to minutes) and follow the cardiac output (Leggett and Williams, 1995) and one model for substances that remain mainly in the blood and are assumed to be distributed according to the relative blood volume of the different organs (ICRP, 2002). There are also standardised models to describe the excretion of substances from the liver to the gastrointestinal tract via the gallbladder, and for bone seeking radionuclides deposited on the surface or in the volume of the trabecular and cortical bone. The two most commonly used standardised models in diagnostic nuclear medicine are the kidney-bladder model and the gastrointestinal tract model (ICRP, 2015). The kidney-bladder model is an age-dependent model assuming that the fraction of excreted activity in the urinary bladder has been eliminated via the kidneys and then voided with an age-dependent fixed interval. The ICRP gastrointestinal tract model (Figure 4) is defined for the Reference Man given in ICRP Publication 23 and gives transfer rates (ICRP, 1979) to be applied on various radiopharmaceuticals which are either administered orally or transferred into the model from other organs.

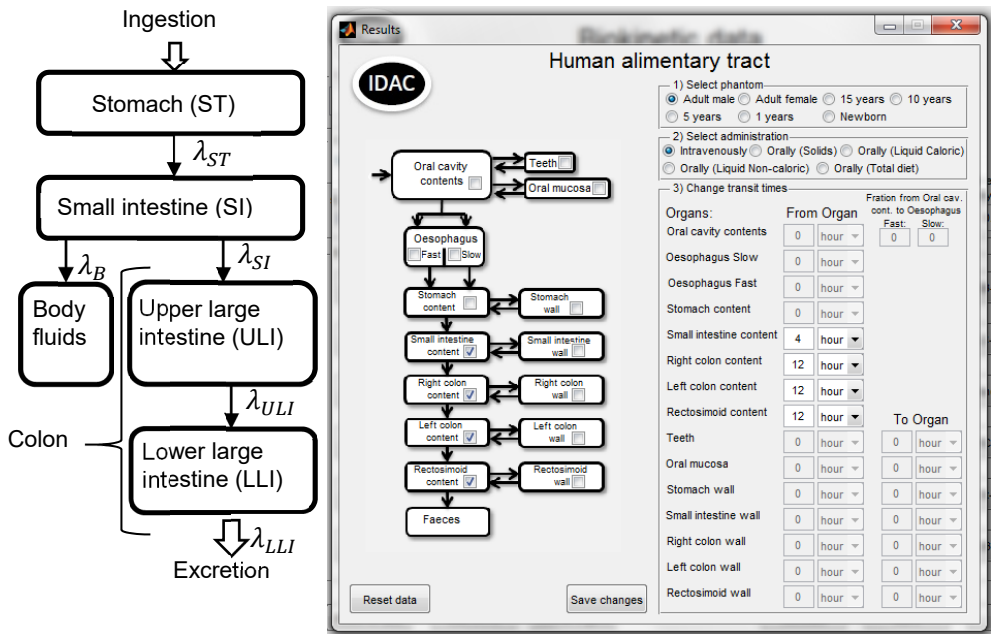


Figure 4. To the left is the former standardised GI-tract model (ICRP, 1980) and to the right is the IDAC2.0 (Paper I) version of the HATM given in ICRP Publication 100.

When ICRP revised the reference person in ICRP Publication 89, the colon was defined in three sections (Left colon, Right colon and Recto-sigmoid colon) instead of the earlier two (Upper large intestine (ULI) and Lower large intestine (LLI)). The new human alimentary tract model presented in ICRP Publication 100 also included mouth and oesophagus together with alternatives due to different types of orally administrated diets and a sex and age dependency. In **Paper I**, the revised HAT model has been incorporated into the internal dosimetry program IDAC2.0 as shown in Figure 4. When revising the biokinetic model for radiopharmaceuticals published by the ICRP the HAT model should replace the former GI-tract model (ICRP, 1979).

The effective dose revision of radiopharmaceutical dosimetry has not yet been performed by the ICRP but others have performed these revisions for the most commonly used radiopharmaceuticals in diagnostic nuclear medicine (Zankl *et al.*, 2012; Hadid *et al.*, 2013; Andersson *et al.*, 2014; 2015). In **Paper V**, five commonly used PET radiopharmaceuticals ^{18}F -fluoride, ^{18}F -fluoroethyltyrosine (^{18}F -FET), ^{18}F -deoxyfluorothymidine (^{18}F -FLT), ^{18}F -fluorocholine, and ^{11}C -raclopride are revised from ICRP Publication 128 to be valid for the updated reference person and compared to the most frequently used PET substance ^{18}F -fluorodeoxyglucose (^{18}F -FDG) (Andersson, 2016). For ^{11}C -raclopride and ^{18}F -FET the cumulated activity in the HAT model was incorporated by mass weighting the different colon structures as:

$$\tilde{A}(r_{\text{Right colon}}, T_D) = 0.71 * \tilde{A}(r_{\text{ULI}}, T_D) \quad (2.5)$$

$$\tilde{A}(r_{\text{Left colon}}, T_D) = 0.29 * \tilde{A}(r_{\text{ULI}}, T_D) + 0.56 * \tilde{A}(r_{\text{LLI}}, T_D) \quad (2.6)$$

$$\tilde{A}(r_{\text{Rectosigmoid colon}}, T_D) = 0.44 * \tilde{A}(r_{\text{LLI}}, T_D) \quad (2.7)$$

where $\tilde{A}(r_{\text{ULI}}, T_D)$ and $\tilde{A}(r_{\text{LLI}}, T_D)$ represent the cumulated activity in the source organs in the previous model, and $\tilde{A}(r_{\text{Right colon}}, T_D)$, $\tilde{A}(r_{\text{Left colon}}, T_D)$, and $\tilde{A}(r_{\text{Rectosigmoid colon}}, T_D)$ are the segmented regions of the new colon tract. The new biokinetic data for the five revised radiopharmaceuticals is presented in Table 1.

Table 1.

Total number of disintegrations per unit of administered activity \tilde{A}/A_0 for ^{11}C -raclopride, ^{18}F -choline, ^{18}F -FET, ^{18}F -FLT, and ^{18}F -fluoride.

Source organ (r_s)	\tilde{A}/A_0 [h]					
	^{11}C -raclopride	^{18}F -choline	^{18}F -FET	^{18}F -FLT	^{18}F -fluoride	^{18}F -FDG
Blood		0.27				
Bone surface					1.4	
Brain	0.11					0.21
Colon contents	0.0028		0.00028			
Gallbladder contents	0.0062					
Heart wall	0.0037					0.11
Kidneys	0.023	0.14	0.023	0.053		
Liver	0.081	0.42	0.093	0.34		0.13
Lungs	0.0073		0.047			0.079
Other organs and tissues	0.27	1.6	2.1	1.7	0.33	1.7
Red bone marrow	0.0098		0.047	0.25		
Small intestine contents	0.023		0.0018			
Small intestine wall	0.019					
Spleen		0.022			0.015	
Urinary bladder contents	0.026	0.10	0.26	0.15	0.030	0.26

In general, there is no consistency on how to estimate the activity in the urine content in the urinary bladder. The ICRP has two different methods: one for occupationally exposed persons where the urinary bladder is assumed to have a first order kinetics with a mean residence time of 2 hours, and one for patients examined with radiopharmaceuticals where the bladder has an age dependent voiding interval and is completely emptied at each void. In biokinetic studies many different voiding intervals are presented in the literature, but the most common are voiding intervals of 2 or 4 hours (Koole *et al.*, 2009; O'Keefe *et al.*, 2009; Lin *et al.*, 2010; Joshi *et al.*, 2014). Figure 5 shows a biokinetic model where the activity is excreted from the blood plasma through the kidneys before entering the urinary bladder and then leaving the body. Independent of the voiding from the urinary bladder, the urinary bladder contents are for dose calculation almost always considered as having a fixed volume with the mass of 50 g for the adult male and 40 g for adult female (ICRP, 2002). Cloutier *et al.* (1973) was first to present a more realistic model with a dynamic urinary bladder which was emptied when it reached 300 mL. In the biokinetic model by Thomas *et al.* (1992; 1999), the contents are instead estimated out of several real physical and biological parameters. The interest in including a dynamic urinary model into

compartmental modelling has been low, probably because the data needed to describe the dynamic urinary bladder contents are patient specific and compartmental modelling for diagnostic examinations are performed on a general population.

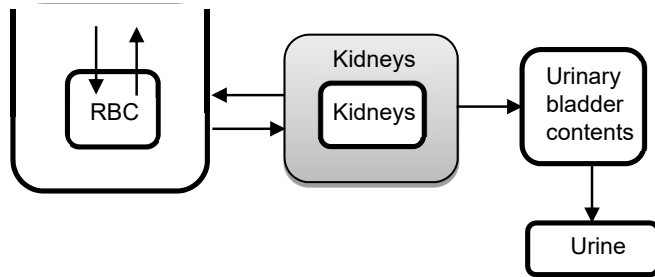


Figure 5. A biokinetic model for indium ions where the substance is excreted through the urinary bladder contents (**Paper VI**).

Systemic compartmental modelling

In order to develop a compartment model for a systemic substance more comprehensive work is required. The systemic model describes the distribution of a radionuclide after it reaches the systemic circulation and its excretion from the human body, instead of assuming an instant organ uptake of the administered activity as is done in the descriptive model described above. The biokinetics of iodide is one of the few radiopharmaceuticals that is described as a systemic model by the ICRP (ICRP, 1986; 2015). ICRP also produces biokinetic models for occupational intake where the biokinetic models of the radioactive elements often are based on systemic models (ICRP, 2015b). The radionuclides used in diagnostic nuclear medicine have usually a much shorter physical half-life compared to those that are of concern for occupational exposure with the consequence that the total number of total disintegrations in the pools are different. For radionuclides with long physical half-life the prediction of the circulating radionuclides will be more accurate using compartmental modelling than descriptive.

In **Paper VI**, a systemic biokinetic model for ionic indium was proposed, which is presented in Figure 6. Compared to the descriptive biokinetic model for ionic indium shown in Figure 3, a systemic model is more complex. It is also a compromise between biological realism and practical considerations such as the quantity and quality of the underlying data.

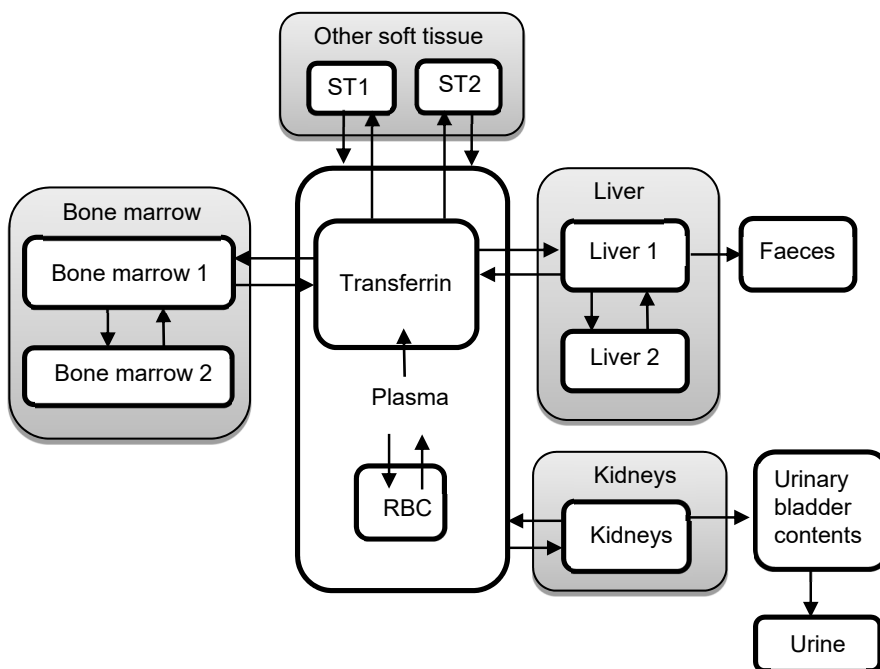


Figure 6.
The proposed biokinetic model for systemic indium presented in **Paper VI**.

The biokinetic model proposed in **Paper VI** (Figure 6) is based on human blood retention and excretion data (Goodwin *et al.*, 1971; Simonsen *et al.*, 2009), but the model for bone marrow, liver, kidneys, and red blood cells are based on various animal studies (Smith *et al.*, 1960; Hosain *et al.*, 1969; Castronovo *et al.*, 1971; 1973; Finsterer *et al.*, 1973; Lilien *et al.*, 1973; Beamish *et al.*, 1974; McIntyre *et al.*, 1974; Glaubitt *et al.*, 1975; Jeffcoat *et al.*, 1978; Sayle *et al.*, 1982; Jönsson, 1991; Yamauchi *et al.*, 1992; Nakai *et al.*, 2000). The biokinetic model for ionic indium is only valid for molecules which bind to transferrin, such as ionic indium (In^{3+}), indium arsenide (InAs), and indium chloride (InCl_3). The model is optimised mainly using the human data. The plasma retention curve is presented as a blue line in Figure 1 and the data from Simonsen *et al.* (2009) is represented by the dashed red line. The biological half-time of the transferrin retention was modelled to 10.5 hours, which is in good agreement with 10 hours given by Goodwin *et al.* (1971). The indium bound to transferrin is transferred of 20 % to bone marrow, 16 % to liver, and the remaining 64 % to two different “other soft tissue” compartments. The blue line in Figure 2 is the proposed indium distribution in the kidneys and the red blood cells. All transfer rates between compartments are given in Table 2. The systemic biokinetic model was generated with a modified version of the compartmental program in **Paper I**, which uses the iterative 4th order Runge-Kutta-Merson method and is shown in Figure 7. When performing a numerical iterative integration, the integration has to account both for the fast and the slow transfer rates in the model. This means that immediately after the

injection, a short integration time step is preferable to account for the fast transfer. After a while the distribution will be dependent on the slow transfer rates and in this case it will be better to change to a longer integration step, to reduce computational time (Leggett *et al.*, 1993).

Table 2.
Parameter values for the systemic model for indium

From	To	Transfer coefficient (d ⁻¹)
Plasma	Transferrin	83
Plasma	RBC	0.415
RBC	Plasma	0.0554
Transferrin	Bone marrow 1	0.316
Transferrin	Liver 1	0.253
Transferrin	ST1	0.427
Transferrin	ST2	0.586
Bone marrow 1	Transferrin	1.10
Bone marrow 1	Bone marrow 2	0.475
Bone marrow 2	Bone marrow 1	0.00831
Liver 1	Transferrin	0.475
Liver 1	Small intestine contents	0.110
Liver 1	Liver 2	0.554
Liver 2	Liver 1	0.00831
Small intestine contents	Colon	6.0
ST1	Plasma	2.37
ST2	Plasma	0.00475
Plasma	Kidneys 1	1.66
Kidneys 1	Plasma	0.0166
Kidneys 1	Urinary bladder contents	0.0268
Urinary bladder contents	Urine	6.86

All biokinetic curves shown in Figure 1 and 2 are decay corrected and valid for all indium isotopes. For indium there are two radioisotopes which are of clinical importance: ¹¹¹In and ^{113m}In. To calculate the total number of disintegrations in each pool consisting of one or more compartments, the nuclide-specific physical decay constant, $-\lambda_{phys}$, is added to the iterative integration. The total number of disintegrations in compartment “Liver” is 8.17 h with 1 MBq ¹¹¹In injected based on the transfer rates given in Table 2. The distribution of ¹¹¹In in “Liver 2” (number 3 in Figure 7) and the cumulated activities are shown in Figure 7. Cumulated activities are often given per intake of Bq or MBq and therefore the total number of disintegration has the same unit as the integration unit (Leggett and Giussani, 2015; ICRP, 2015).

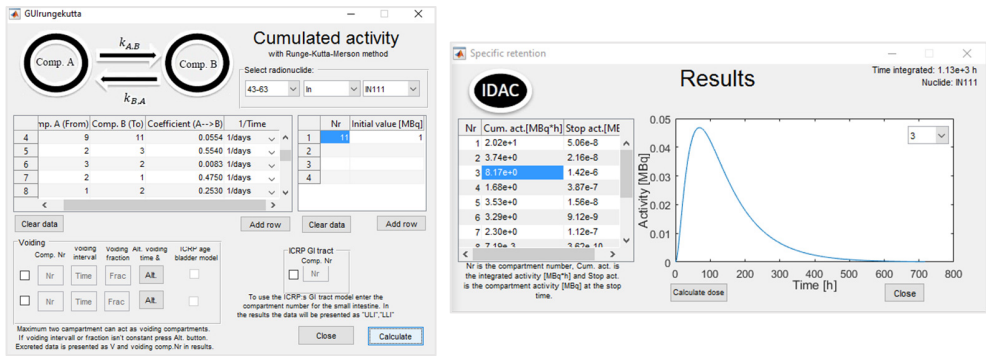


Figure 7. To the left, the biokinetic model with transfer coefficients for ^{111}In . To the right, the cumulated activities for all separate compartments and the time dependent curve for “Liver 2” (Nr 3) (Paper I).

The model determines the spatial and temporal distribution of the decays within the created system. Biokinetic models may also be used to determine the energy deposition for all decays in order to estimate possible biological effects. In compartmental modelling, the defined pools may be arbitrary, but in order to estimate a risk they have to correspond to the organs or tissues, referred to as source regions, which defines the ICRP Reference Person from reference values given in ICRP Publication 23 or 89 (ICRP, 1975; 2002). Therefore, a pool will hereafter be called a source region, r_s .

Chapter 3

Internal dose calculations

Internal dosimetry calculations are motivated by the assumption that the absorbed dose in an organ is a good predictor for biological effect at least at certain dose levels and dose rates (Noßke *et al.*, 2012).

The absorbed dose D is defined in a point as (ICRU, 2011):

$$D = \frac{d\bar{E}}{dm} \quad (3.1)$$

where $d\bar{E}$ is the mean energy imparted to matter of mass dm by ionising radiation. The SI unit is J kg^{-1} and is most often referred to as gray (Gy). In theory, the mean energy imparted is deposited over an infinitesimal volume, but in practise the mean energy imparted is calculated over a finite volume. This volume is called the target region (or tissue), r_T , (Bolch *et al.*, 2009) resulting in a calculation of the mean absorbed dose, \bar{D} . The most common method to calculate absorbed dose from an internally deposited radionuclide is to use the framework provided by the MIRDC Committee of the Society of Nuclear Medicine in USA. The scheme was originally published in 1968 (Loevinger and Berman, 1968) with a latest revision of the MIRDC formalism given in MIRDC pamphlet 21 (Bolch *et al.*, 2009). The MIRDC pamphlet 21 states that the mean absorbed dose for a time-independent system is calculated as:

$$D(r_T, T_D) = \sum_{r_s} \tilde{A}(r_s, T_D) S(r_T \leftarrow r_s) \quad (3.2)$$

where $\tilde{A}(r_s, T_D)$ is the time-integrated activity, *i.e.* the total number of disintegrations, in source region r_s from the time of administration to the time T_D . $S(r_T \leftarrow r_s)$ is the mean absorbed dose in target r_T per nuclear transformations in source region r_s and defined as:

$$S(r_T \leftarrow r_s) = \sum_i \Delta_i \Phi(r_T \leftarrow r_s, E_i) \quad (3.3)$$

where $\Phi(r_T \leftarrow r_s, E_i)$ is the absorbed fraction from the source region r_s to the target region r_T divided by the mass in kilograms of the target region r_T of the i th component in the decay scheme and $\Delta_i = E_i Y_i$ is the energy yield where Y_i is the yield and E_i is the mean energy of the i th nuclear transition of the radionuclide in joule. There are many different databases which tabulate nuclide-specific energies and the corresponding yields but the calculations presented here are all based on the nuclear decay data presented in ICRP Publication 107 (ICRP, 2008b). The MIRDC formalism is a general formalism which can be used for both diagnostic and therapeutic nuclear medicine and be applied on whole

organs, tissue subregions, voxelised structures, and individual cellular compartments. The limiting factor is that there has to be a known absorbed fraction between the source and target regions for a requested radiation type and its corresponding energy. The use in therapeutic nuclear medicine often needs more detailed and individual information about anatomy and absorbed fractions than applications in diagnostic nuclear medicine.

Anatomical models

There are many different phantoms which can be used to simulate absorbed fractions between source and target regions (Xu and Eckerman, 2009). These mathematical models can be divided into three different generations: stylised, voxelised, and non-uniform rational B-spline phantoms. In each new generation, structures and features are increasingly realistic and detailed for use in Monte Carlo simulations to generate more accurate absorbed fractions. Monte Carlo simulations are performed on the mathematical models and the absorbed doses are hence calculated for target regions defined by the phantoms.

Stylised

The first generation phantoms are stylised mathematical models described by linear and quadratic equations. The most commonly used phantom in diagnostic nuclear medicine for estimation of absorbed doses to various organs and tissues is the adult phantom by Snyder *et al.* (1974). This was later improved and completed with phantom for other ages by Cristy and Eckerman (1987). These phantoms have been used in the ICRP publications and in biokinetic dosimetry programs (Johansson 1985; Stabin *et al.*, 2005; Andersson *et al.*, 2012). The mathematical models are very schematic. For the family phantoms by Cristy and Eckerman, the source regions (phantom structures) are defined based on the Reference Man defined in ICRP Publication 23 (ICRP, 1975), which is described as a Caucasian Western European or North American person. The ICRP stresses that the Reference Man does not represent a random sample of any specified population (ICRP, 1975).

Voxel

The second generation phantoms are the voxel based mathematical models derived from high-resolution computed tomography images or magnetic resonance imaging of real humans. The human images have been voxelised and all voxels have been segmented and given an object identifier number (OID), where every OID represent a source region. There have been many voxelised phantoms created for different purposes, but they are all derived from the images of one individual person (Xu and Eckerman, 2009).

Non-uniform rational B-spline

The third generation phantoms are the non-uniform rational B-spline phantoms which are based on mathematical models that use a set of control points to define surfaces. This gives the possibility to modify or introduce anatomical differences in size or describe other characteristics as, for example, a mathematical model generated to simulate respiratory motion (Segars *et al.*, 2010).

ICRP/ICRU adult reference phantoms

The adult male and adult female ICRP/International Commission on Radiation Units and Measurements (ICRU) computational voxel phantoms were approved by ICRP in 2007 and adopted by ICRU in 2008 as reference phantoms for dosimetric calculations (ICRP, 2009). These mathematical models were constructed by adjusting the voxel phantoms of Golem (Zankl *et al.*, 2001) and Laura (Zankl *et al.*, 2005) to the organ masses given in the ICRP Publication 89 (ICRP, 2002) and are shown in Figure 8. The phantoms are published in ICRP Publication 110, and also available in digital format as a big text file with 143 different OIDs. From this digital phantom file, the voxel phantoms have been incorporated into the IDACSTAR computer program (**Paper III**). The male reference phantom is composed of 1.95 million voxels where each voxel has an axial size of $2.137 \times 2.137 \text{ mm}^2$ and a height of 8.0 mm. The female reference phantom is composed of 3.89 million voxels where each voxel has an axial size of $1.775 \times 1.775 \text{ mm}^2$ and a height of 4.84 mm, meaning that the female phantom has a higher spatial resolution (better defined structures than the male phantom). Unlike the previous mathematically described models, specific-absorbed fraction (SAF) values for electrons may now also be simulated using Monte Carlo methods and have been published by Zankl *et al.* (2012). The SAF values presented in the study of Zankl *et al.* (2012) have been incorporated into the internal dosimetry program IDAC2.0 (**Paper I**). SAF values are published for 63 source regions and 67 target region and for 25 monoenergetic photons and electrons ranging from 10 keV to 10 MeV.

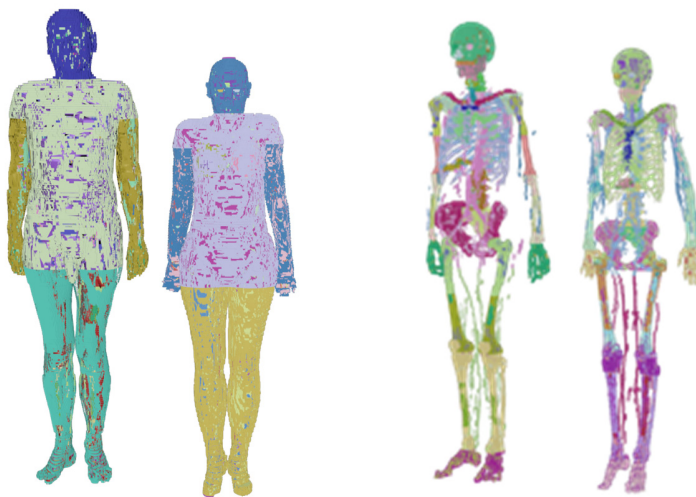


Figure 8.

The ICRP/ICRU adult male (left) and female (right) reference voxel phantoms. For the right pair, all object identifier numbers (OID) are shown and for the left only a few selected OIDs are shown.

Specific absorbed fraction values

Monte Carlo simulated specific absorbed fraction values represent the fraction of energy transferred from a source region to a target region divided by the mass of the target region. Normally a uniform activity concentration within the source region is assumed for the simulations. Absorbed dose is the mean energy deposition registered within the whole target region divided by its mass. The radiation emitted as consequence of a nuclear transformation is radionuclide dependent, and in ICRP Publication 107 radiation from 1252 radionuclides are listed (ICRP, 2008b). SAF values may be presented in tables for monoenergetic photons and electrons. From these tables the SAF values for the radiation components emitted from a specific radionuclide can be derived through interpolation. In **Paper III**, SAF values from the radionuclides in urine bladder contents source region to the urinary bladder wall target region were simulated for different urine contents volumes (Figure 9).

Specific absorbed fractions of energy (1/kg)
Adult Male Reference Computational Phantom

Photons

Vol.	Traget <-Source	0.010	0.015	0.020	0.030	0.040	0.050	0.060	0.080
10mL	UB-wall<-UB-cont	2.028E+00	5.550E+00	6.644E+00	4.184E+00	2.416E+00	1.596E+00	1.206E+00	9.115E-01
50mL	UB-wall<-UB-cont	1.172E+00	2.837E+00	3.379E+00	2.329E+00	1.427E+00	9.744E-01	7.466E-01	5.673E-01
100mL	UB-wall<-UB-cont	8.995E-01	1.932E+00	2.241E+00	1.617E+00	1.030E+00	7.191E-01	5.566E-01	4.256E-01
150ml	UB-wall<-UB-cont	7.553E-01	1.500E+00	1.705E+00	1.266E+00	8.285E-01	5.860E-01	4.586E-01	3.513E-01

Figure 9.

Monoenergetic SAF values at different energies for different volumes of the urinary bladder contents as a source region to the urinary bladder wall (**Paper III**).

Absorbed dose calculations

The mean absorbed dose as defined in equation 3.2 is calculated by summing the dose contribution from all source regions to a specific target region. The total number of transformations in the source regions with energy and yield for each radiation component together, multiplied with the corresponding SAF values are gives the absorbed dose to the target region. The calculation is often straightforward, but may be extensive in cases of many separate nuclear transitions with disintegrations in several source regions connected to many target regions. Therefore, the absorbed dose calculations will be facilitated if they are automated in a computer program. Figure 10 shows the user interface of the absorbed dose calculation program presented in **Paper I**. In this program the user can select a radionuclide defined in the ICRP Publication 107 and insert the cumulated activities for the estimated source regions. The computer program then calculates the absorbed dose to the target regions defined by Zankl *et al.* (2012) which were simulated using the ICRP/ICRU reference phantoms.

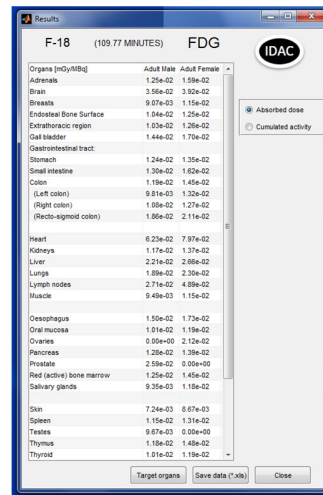
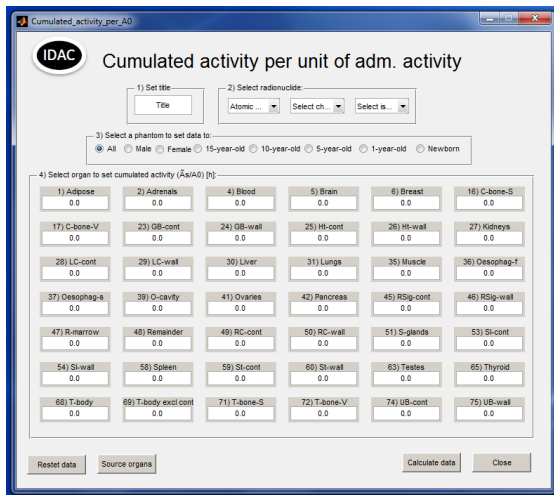


Figure 10.

The internal dose computer program developed in **Paper I**, where the absorbed and effective doses are calculated out of predefined SAF values (Zankl *et al.* 2012). The program is here presented for ^{18}F -FDG.

Using this program, absorbed doses were calculated for both adult males and females for the proposed model of systemic indium in **Paper VI**. The calculated absorbed doses per intravenously administered activity are presented in Table 3 for ^{111}In and $^{113\text{m}}\text{In}$. The effective dose is also calculated for both isotopes and are also compared with the results of earlier biokinetic models published by ICRP.

Table 3.

Absorbed doses (mGy/MBq) and the effective dose (mSv/MBq) per administered activity for the proposed indium model in **Paper VI** compared with the calculated effective dose from the biokinetic indium models presented in the ICRP Publication 53 and 72 as calculated by the computer program developed in **Paper I**.

Organs	¹¹¹ In		^{113m} In	
	Adult Male [mGy/MBq]	Adult Female [mGy/MBq]	Adult Male [mGy/MBq]	Adult Female [mGy/MBq]
Adrenals	3.80E-01	4.81E-01	1.49E-02	1.70E-02
Brain	9.93E-02	1.15E-01	2.92E-03	3.26E-03
Breasts	1.27E-01	1.60E-01	5.30E-03	6.79E-03
Endosteal Bone Surface	1.42E-01	1.74E-01	3.78E-03	4.27E-03
Extrathoracic region	1.09E-01	1.44E-01	6.92E-03	7.97E-03
Gallbladder	4.54E-01	5.33E-01	1.36E-02	1.64E-02
Gastrointestinal tract:				
Colon	2.25E-01	2.35E-01	1.48E-02	1.49E-02
Small intestine	2.27E-01	2.72E-01	1.48E-02	1.64E-02
Stomach	2.76E-01	3.16E-01	1.54E-02	1.68E-02
Gonads	1.06E-01	2.04E-01	3.48E-03	6.37E-03
Heart	2.92E-01	3.39E-01	1.09E-02	1.33E-02
Kidneys	5.58E-01	6.34E-01	3.02E-02	3.39E-02
Liver	6.39E-01	7.57E-01	2.02E-02	2.46E-02
Lungs	2.82E-01	3.31E-01	2.32E-02	2.83E-02
Lymph nodes	3.46E-01	5.91E-01	1.13E-02	1.62E-02
Muscle	1.15E-01	1.43E-01	2.58E-03	3.21E-03
Oesophagus	2.90E-01	3.34E-01	1.69E-02	1.92E-02
Oral mucosa	1.02E-01	1.27E-01	2.25E-03	3.02E-03
Pancreas	3.55E-01	3.79E-01	1.54E-02	1.70E-02
Prostate/Uterus	1.64E-01	2.06E-01	7.81E-03	9.88E-03
Red (active) bone marrow	2.17E-01	2.60E-01	6.38E-03	6.88E-03
Salivary glands	1.10E-01	1.43E-01	7.42E-03	8.83E-03
Skin	7.85E-02	9.53E-02	2.72E-03	3.52E-03
Spleen	2.91E-01	3.35E-01	2.51E-02	2.80E-02
Thymus	2.03E-01	2.49E-01	1.07E-02	1.30E-02
Thyroid	1.63E-01	1.91E-01	8.84E-03	1.03E-02
Urinary Bladder	1.44E-01	1.58E-01	2.60E-03	3.53E-03
Effective dose	2.53E-01 mSv/MBq		1.27E-02 mSv/MBq	
Effective dose (ICRP 72)	2.60E-01 mSv/MBq		6.29E-03 mSv/MBq	
Effective dose (ICRP 53)	1.80E-01 mSv/MBq		6.23E-03 mSv/MBq	

Fixed urinary bladder volume

The urinary bladder wall is considered to be a radiosensitive organ for inducing cancer later in life. The absorbed dose to the urinary bladder wall depends on which voiding interval is used. The most conservative assumption is to assume no voiding at all, meaning that all activity which is transferred to the urinary bladder also decays in the urinary bladder. The absorbed doses to the urinary bladder wall were compared between different voiding intervals in **Paper V** (Figure 12). The absorbed doses are presented for a ^{18}F -fluoride examination calculated assuming various urine voiding intervals ranging from 1 to 6 hours. There is a wide variety in absorbed dose depending on voiding interval, and therefore, a consensus on a suitable voiding time when performing general dose estimations to a population would be preferable. If examinations are optimised after population-based absorbed dose calculations, the assumption of voiding interval could have a real impact on the image quality and hence have a possible effect on diagnostic outcome. Therefore, examinations should be optimised on other criteria.

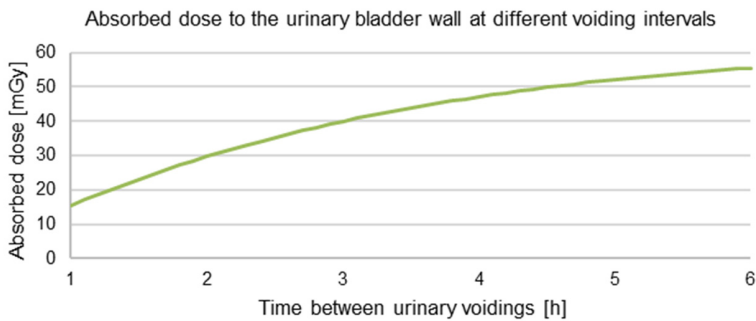


Figure 12. The absorbed dose to the urinary bladder wall from a 300 MBq administration of ^{18}F -fluoride calculated with different constant voiding intervals based on the data given in ICRP Publication 128 (2015) (**Paper V**).

Dynamic urinary bladder volume

In **Paper III**, absorbed dose calculations are performed based on the SAF values presented in Figure 9 using the method to estimate the volume of a dynamic urinary bladder described by Thomas *et al.* (1992; 1999). The estimations were performed using the data presented in Table 1 in **Paper III**. For a $^{99\text{m}}\text{Tc}$ -mercaptoacetyl triglycine (MAG3) examination the absorbed dose to the urinary bladder wall was calculated to 0.09 mGy/MBq for males and 0.10 mGy/MBq for females. The use of volume dependent SAF values instead of fixed SAF values will result in higher absorbed dose. The assumption behind calculating absorbed doses to the urinary bladder wall where the SAF values changes with the urine content in the bladder are to simulate spherical bladder contents and bladder wall. The contents size depends only on the urine volume and the outer wall has a fixed mass. For volumes larger

than the fixed urinary bladder the SAF values will be lower and for smaller volumes the SAF values will be higher because of self-absorption within the contents itself for a uniform distributed activity. For the parameters given in Table 1 in **Paper III** the volume of the urinary bladder will mostly be smaller than the fixed geometry. The results of 11 different biokinetic models were compared in **Paper III** and are shown in Figure 13 together with the time dependent urinary bladder volume, the activity in the urinary bladder and the interpolated dynamic SAF values for ^{99m}Tc -MAG3 for the male phantom.

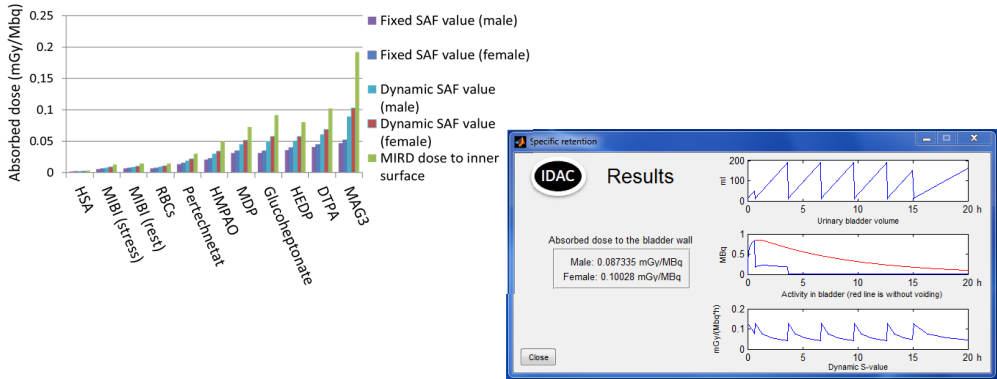


Figure 13. Absorbed dose to the urinary bladder wall for 11 cases to the left and to the right is the urinary bladder volume, the activity in the contents and the dynamic SAF from 0 to 20 hours after an ^{99m}Tc -MAG3 examination. The red line is the hypothetical activity in the bladder without any voiding (**Paper III**).

Sources of uncertainty in internal dosimetry

All data and results include uncertainties. The relevance of these uncertainties is dependent on the application of the dosimetric data. When using ^{177}Lu peptides for radionuclide therapy, the kidneys are the limiting organs at risk. Kidney dose estimates based on patient-specific calculations have a reported uncertainty of 6 % (1 SD) (Gustafsson *et al.*, 2015). In diagnostics, however, the calculations are based on biokinetic population models, so the question is how well they represent a specific individual. Roedler (1980) showed that using reference phantoms and population-based biokinetic models will estimate the real patient dose within a factor of 3, and within a lower factor for radionuclides with short half-life *e.g.* ^{99m}Tc . The general proposed uncertainty is a factor of 2 or greater (Svegborn, 1999; Zanzonico, 2000; Norrgren *et al.*, 2003; Stabin, 2008b). Other relevant questions are how well the biokinetic models and the mathematical anatomical models represent the general populations. The mathematical anatomical models are defined for a western Caucasian population. The tissue weighting factors given in ICRP Publication 103 for radiation-induced biological effects are defined for all populations, ages, and sexes. Thus, applying these factors on individuals or subgroups is incorrect and therefore this uncertainty is irrelevant. The uncertainties in the tissue weighting factors are not within the scope of this work.

The uncertainties of biokinetic modelling of indium for an age and sex independent population are unknown. The data points used to generate the indium model in **Paper VI** are obtained from published papers and they were often presented as mean values without any uncertainty estimation. The model is based on data gathered from small animals, *e.g.* rats and mice, dogs, as well as for humans. The biokinetic model was constructed by fitting the model to the mean plasma retention curve for 15 healthy subjects. The initial indium transfers between various organs and tissues will mostly be blood dependent and the uncertainty in the presented absorbed doses will probably be within the factor of 3 or less (Roedler, 1980) for the clinically used ^{111}In - and $^{113\text{m}}\text{In}$ -ions. For long-lived indium isotopes there are still not enough data available to construct a biokinetic model. After about 100 days the erythrocytes dies and indium is recycled. The uncertainties in the long-term fitting to the model are difficult to estimate. For other elements there have been various versions of the biokinetic model to account for population-based uncertainties (Pawel *et al.*, 2007), but there is still not enough data to perform this on indium.

Biological effects

It is well known that ionising radiation has a biological effect on the human body. There are two types of harmful effects: deterministic (tissue) effects and stochastic effects (ICRP, 2007).

Deterministic effects

A deterministic effect is often of an acute nature and caused by high doses. The deterministic effects are characterised by a threshold dose after which the effect increases in severity as the dose is further increased. Situations when the dose threshold for deterministic effects in relevant organs could be exceeded should under almost all circumstances be subject for protection actions (ICRP, 2007). This thesis is concerned with stochastic effects and the results should not be applied to estimate any deterministic effects.

Stochastic effects

Stochastic effects are caused by both high and low doses, and are effects observed as a statistically detectable increase in the incidence of cancer or heritable disease occurring a long time after exposure. To estimate the biological effect from a disintegration there are two correction factors, the radiation weighting factor, w_R , and the tissue weighting factor, w_T , applied on the mean absorbed dose. The radiation weighting factors are defined largely to reflect the relative biological effectiveness for stochastic effects of different types of radiation. In diagnostic nuclear medicine $w_R = 1$ is used for all radiation types. The

tissue weighting factor is defined to reflect the relative contribution from the organ and tissue to the total detriment for stochastic effects, which is the total harm to health experienced by an exposed group and its descendants. The tissue weighting factors published in ICRP Publication 103 given in Table 4 are sex- and age- averaged values and it is stressed that the application of these factors are restricted to the effective dose definition and not used for the assessment of individual risk.

Table 4.
Tissue weighting factors w_T for 13 different organs (ICRP, 2007).

Organ	w_T	Organ	w_T	Organ	w_T
Breast	0.12	Gonads	0.08	Bone surface	0.01
Colon	0.12	Bladder	0.04	Brain	0.01
Lung	0.12	Oesophagus	0.04	Salivary glands	0.01
Stomach	0.12	Liver	0.04	Skin	0.01
Remaining tissues*	0.12	Thyroid	0.04		

*Remaining tissues: Adrenals, extrathoracic (ET) region, gallbladder, heart, kidneys, lymphatic nodes, muscle, oral mucosa, pancreas, prostate (♀), small intestine, spleen, thymus, and uterus/cervix (♂).

Effective dose calculations

The effective dose is a radiation protection quantity defined by the ICRP to estimate the total harm to health experienced by an exposed group and its descendants caused by stochastic effects. The quantity was first introduced in the ICRP Publication 26 and a year later the term ‘effective dose equivalent’ and the symbol ‘ H_e ’ were assigned for this new concept. Up to now ICRP has revised the weighting factors twice and also changed the name of the quantity to effective dose (E) (ICRP, 1977; 1978; 1991; 2007). The unit is sievert (Sv). There is an ongoing discussion related to the need to describe the advantages and limitations of effective dose in more detail (Harrison *et al.*, 2016)

Effective dose is calculated from the equivalent dose. The equivalent dose is the absorbed dose multiplied with the radiation weighting factors w_R . For beta and gamma radiation the w_R is equal to 1. The effective dose is then calculated as the sum of the organs tissue weighting factors multiplied by the arithmetic mean of the sex-specific equivalent dose of for each of the corresponding organs:

$$E = \sum_T w_T \sum_R \frac{w_R D_R(r_T, T_D)_{male} + w_R D_R(r_T, T_D)_{female}}{2} \quad (3.4)$$

where w_T is the tissue weighting factor for tissue T and $\sum_R w_R D_R(r_T, T_D)_{sex}$ is the sex-specific equivalent dose for target region r_T .

In **Paper IV**, the effective dose was estimated for ^{18}F -fluoride, ^{18}F -FET, ^{18}F -FLT, ^{18}F -choline, and ^{11}C -raclopride, and the results are presented in Table 5.

Table 5.

The effective dose from ¹⁸F-FDG*, ¹⁸F-fluoride, ¹⁸F-FET, ¹⁸F-FLT, ¹⁸F-choline, and ¹¹C-raclopride and the difference in % compared to the effective dose presented in ICRP Publication 128 (**Paper IV**).

Radiopharmaceutical	This Study [mSv/MBq]	Difference [%]
¹⁸ F-FDG	1.7E-02*	-11
¹⁸ F-Fluoride	8.9E-03	-48
¹⁸ F-FET	1.5E-02	-6
¹⁸ F-FLT	1.4E-02	-7
¹⁸ F-choline	2.0E-02	0
¹¹ C-raclopride	4.3E-03	-14

*Andersson *et al.*, (2015)

Paper V is a review paper on dose management and presents other previously (Andersson *et al.*, 2014; 2015) revised effective dose calculations for twelve clinically relevant radiopharmaceuticals, all shown in Figure 14.

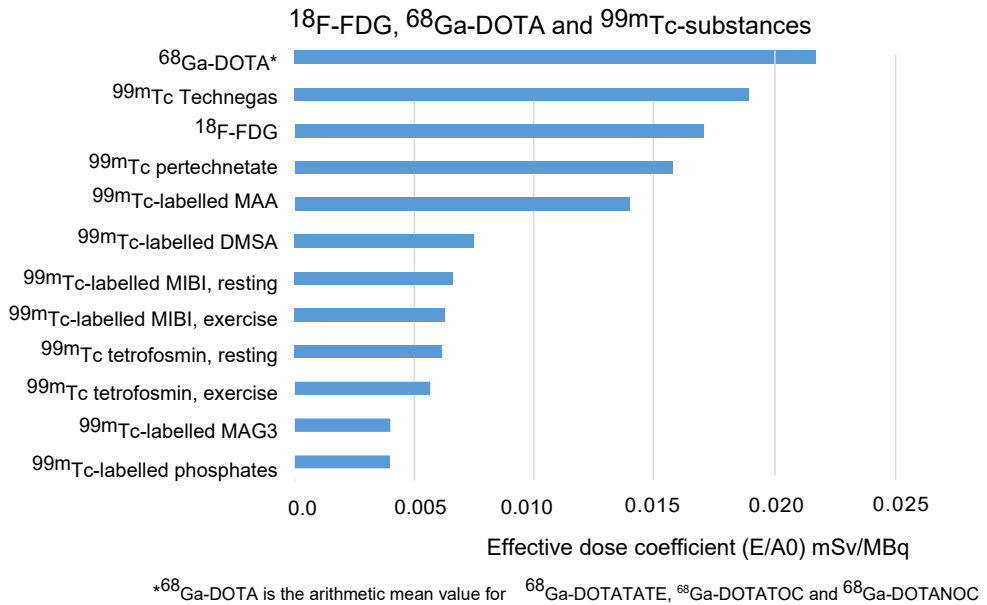


Figure 14.

The effective dose per MBq for twelve clinically relevant and frequently used radiopharmaceuticals (**Paper V**).

The effective dose is estimated to a Reference Person and is generated from absorbed dose calculations to the Reference Male and Reference Female. In **Paper II**, where customised dose calculations were performed on the Reference Individuals, simulations also included sex-specific organs *e.g.* ovaries. By definition, effective dose estimation may not be performed if absorbed doses are known for only one of the two Reference Individuals which defines the Reference Person. Therefore, a new quantity was defined in **Paper IV** and named “component dose”. There could be a use for the component dose quantity even if it is formally an incorrect use of the tissue weighting factors. The reason of introducing this new quantity is to avoid undermining the effective dose quantity by using it for estimations it is neither intended nor defined for.

Chapter 4

Summary of papers

Paper I: Internal radiation dosimetry computer program, IDAC 2.0, for estimation of patient doses from radiopharmaceuticals

Paper I describes an updated version of the internal dosimetry computer program called “Internal dose assessment by computer” (IDAC), which was created to facilitate effective dose and absorbed dose calculations for organs and tissues for use in diagnostic nuclear medicine. The new version, IDAC2.0, incorporates the ICRP/ICRU adult reference voxel phantoms and decay data from ICRP Publication 107. Performing dose calculations on the SAF values based on the voxel phantoms allows biokinetic modelling of the ICRP human alimentary tract model and effective dose calculations based on the updated tissue weighting factors given in ICRP Publication 103. The introduction of the HAT model in the program allows modelling of the transport of orally administered radiopharmaceuticals, which previously were modelled to start in the stomach. The effective dose was calculated for 34 orally administered radiopharmaceuticals.

Paper II: IDACSTAR: a MCNP application to perform realistic dose estimations from internal or external contamination of radiopharmaceuticals

In **Paper II**, a Monte Carlo based stand-alone program was created called IDACSTAR. The main purpose of the program is to create Monte Carlo simulation input files for MCNP to facilitate absorbed dose and effective dose estimations from customisable SAF values and arbitrary source regions. The program also allows easy estimation of effective dose from skin contaminations. IDACSTAR is a graphical user interface where the user defines the activity in the voxel phantoms. For three predefined radionuclides, ^{18}F , $^{99\text{m}}\text{Tc}$ and ^{131}I , the program performs automatic simulations of absorbed doses to organs and tissues and calculates the effective dose. The program has been applied on a hypothetical skin contamination case with $^{99\text{m}}\text{Tc}$, and on a real clinical extravasation case of a patient examined with ^{18}F -FDG.

Paper III: Improved estimates of the radiation absorbed dose to the urinary bladder wall

In **Paper III**, sex-specific monoenergetic photon and electron dynamic SAF values are simulated ranging for the source region urinary bladder contents to the target regions bladder wall and contents with simulated urinary bladder contents ranging from 10 mL up to 800 mL. The resulting SAF values are based on a spherical bladder model and the anatomical and physiological data is based on the ICRP Publication 89. The generated SAF values are used to calculate the absorbed dose to the urinary bladder wall for two

radiopharmaceuticals: ^{18}F -FDG and $^{99\text{m}}\text{Tc}$ DTPA. The results show that using SAF values for a dynamic urinary volume, rather than fixed, will lead to a higher absorbed dose to the urinary bladder wall due to the smaller dynamic bladder volume compared to the fixed model. The smaller volume causes less attenuation in the bladder contents itself and thus higher SAF values and a higher absorbed dose to the urinary bladder wall.

Paper IV: Organ doses and effective dose for five PET radiopharmaceuticals

In **Paper IV**, the absorbed doses and effective doses are calculated for five radiopharmaceuticals intended for PET-examinations, using the computer program IDAC2.0 presented in **Paper I**. Diagnostic PET-examinations are dominated by the use of ^{18}F -FDG, but there are other relevant radiopharmaceuticals commercially available or under development. For five of these radiopharmaceuticals, ^{18}F -fluoride, ^{18}F -fluoroethyltyrosine (^{18}F -FET), ^{18}F -deoxyfluorothymidine (^{18}F -FLT), ^{18}F -fluorocholine (^{18}F -choline), and ^{11}C -raclopride, the effective dose is calculated to estimate the potential risk of stochastic effects for a representative population. The biokinetic models were obtained from ICRP Publication 128 and tissue weighting factors were taken from ICRP Publication 103. The estimated effective dose in mSv MBq^{-1} was 0.015 for ^{18}F -FET, 0.015 for ^{18}F -FLT, 0.020 for ^{18}F -choline, 0.0090 for ^{18}F -fluoride, and 0.0044 for ^{11}C -raclopride. For specific organ absorbed doses there are in some cases substantial differences to earlier estimation, but the effective dose was significantly different only for ^{18}F -fluoride, for which a dose reduction of 48 % was calculated using the IDAC2.0.

Paper V: Dose management in conventional nuclear medicine imaging and PET

Paper V is a review of the basic concepts of dose management in PET and conventional nuclear medicine imaging. The amount of activity administered in a nuclear medicine investigation determines the image quality and to a certain degree the diagnostic accuracy, but there are only a few studies trying to find an optimum activity. The paper states that nuclear medicine is far behind on image acceptable quality criteria and visual grading analysis compared to *e.g.* diagnostic radiology. The establishment of diagnostic reference levels is used as a method towards more optimal investigations in nuclear medicine. The main contribution of **Paper V** is the recommendation to adjust the administered activity by the patient's weight. One of the keys to a successful dose management is continuous education and training of all staff categories involved in patient examinations.

Paper VI: A biokinetic model and absorbed doses for systemic indium

In **Paper VI**, a proposed systemic model of indium is presented. The model is based on both human and animal data, published between 1960 and 2016, for ionic indium, indium chloride, and indium arsenic which all has a strong binding to transferrin. The model consists of five different pools defined by 10 specific compartments and 21 specified transfer rates. The indium bound to transferrin is assumed to have a biological half-time of 10.5 hours. Absorbed doses and effective doses are calculated for ^{111}In and $^{113\text{m}}\text{In}$. Revised effective dose calculations are also performed on the two previous indium models presented by the ICRP. Although the presented model still lacks sufficient reliable human data to

completely describe the distribution of indium in humans, it is likely a more correct biokinetic model in comparison to the published ICRP indium models which are both based on animal data only.

Chapter 5

Discussion and future outlook

The aim of this thesis was to improve radiation dose estimations for nuclear medicine examinations of patients. The improvement has been achieved by implementation of the new ICRP anatomical and voxelised mathematical models for adults, awaiting the models for paediatric patients. Concerning the necessary and equally important biokinetic models there is still much to do (Mattsson, 2015). Biokinetic modelling needs repeated quantitative measurements on patients/volunteers using the most advanced imaging equipment. The current trend is unfortunately the opposite, as exemplified by the dosimetry for amyloid binding radiopharmaceuticals (Scheinin, *et al.*, 2007; O'Keefe *et al.*, 2009; Koole *et al.*, 2009; Lin *et al.*, 2010; Pontecorvo *et al.*, 2014). For these radiopharmaceuticals the biokinetic models are based on fewer subjects and time points than what has been common practice for earlier developed substances. The explanation might be that biokinetic studies are time consuming and requires several additional measurements on already heavily booked clinical imaging equipment. Today's economy-driven health care leaves less and less room for this kind of clinical research. Important future projects would be to collect biokinetic information from a sufficient number of subjects for a specific radiopharmaceutical so that sex- and age-specific biokinetic model can be developed. It is highly desirable to get enough data to be able to construct biokinetic compartment models which describe the radionuclide transfer between various organs and circulating blood. In the specific absorbed fractions for the ICRP reference phantoms (ICRP, 2016) there is a specific source region defined for the circulating blood, hopefully allowing more biokinetic models to include a blood compartment in the future.

The small risk to later in life develop a radiation-induced cancer from a diagnostic radiopharmaceutical is currently estimated using the quantity effective dose. The radiation weighting factors used to estimate the effective dose is set to 1 for photons and electrons from radionuclides in diagnostic nuclear medicine. However, for very low energy electrons like those from Auger electron emitters (like ^{51}Cr , ^{67}Ga , $^{99\text{m}}\text{Tc}$, ^{111}In , and others) and bound to DNA, ICRP acknowledges that a larger radiation weighting factor may be appropriate, even if no specific value is recommended. Humm *et al.* (1994) recognised that DNA-incorporated radionuclides emitting Auger electrons have a similar effect as α -particles and recommends a radiation weighting factor of 20 for stochastic effects and 10 for deterministic effects. These factors are hence given for subcellular distributions, which if taken into account *e.g.* by compartmental modelling of the intracellular radionuclide distribution, may have an impact on the effective dose. The subcellular distribution and microdosimetry could be of high importance for risk estimations.

There is also a need to improve the estimation of stochastic effects for various population groups. One reason for this is the sex, age, and population unspecific nature of the effective dose protection unit (ICRP, 2007). It is questionable how well the data of the Life Span Study applies to the exposure situations in diagnostic nuclear medicine. The current risk estimates assume a linear no-threshold dose/risk model and a dose and dose rate effectiveness factor. Epidemiological studies based on dose data generated today and during the next decades are needed to improve risk estimations for stochastic effects.

An interesting future possibility is complete and automated segmentation of organs and structures in the CT- or MR-images from each individual patient. This will facilitate individual absorbed dose estimations and might, combined with a dose tracking system, generate sufficient epidemiological data for more accurate predictions of stochastic effects. In addition, specific subgroups based on physiological parameters may be identified, and form the basis for more specific biokinetic models. On the other hand, future development of tracers based on radionuclides with short physical half-lives, *i.e.* from seconds or up to a few minutes, would make individual differences minimal and general biokinetic models would likely be sufficient.

In the coming years the ICRP will also publish ten paediatric mathematical anatomical models together with mathematical models of an adult pregnant female and her developing embryo/foetus at different stages during her pregnancy. The implementation of these mathematical models into nuclear medicine will be much less time consuming using the framework presented in this thesis.

Chapter 6

Conclusions

The work underlying this thesis has led to the following conclusions:

- Absorbed dose calculations for a specific radiopharmaceutical in diagnostic nuclear medicine can be automated for more detailed mathematically voxelised reference models.
- Revision of descriptive models to systemic biokinetic models will provide more realistic biokinetic models.
- Effective dose estimations dedicated for diagnostic nuclear medicine based on the definitions in ICRP Publication 103 can be performed with the new anatomical mathematical models and the modified biokinetic models using the software developed in this thesis.
- Voxelised mathematical models creates possibilities to develop new methods to calculate the absorbed dose and facilitates dose estimation in subregions such as part of the skin, kidneys, or brain.
- A dynamic urinary bladder model provides more degrees of freedom and likely results in more realistic absorbed dose estimation than the reference mathematical models, which assume a fixed volume of the urinary bladder.

Bibliography

- Andersson, M., Johansson, L., Minarik, D., Mattsson, S., Leide-Svegborn, S. An upgrade of the internal dosimetry computer program IDAC. In: Medical Physics in the Baltic States 10. (Ed. by D. Adlenè), Kaunas University of Technology 2012 120-123.
- Andersson, M., Johansson, L., Minarik, D., Leide-Svegborn, S., Mattsson, S. Effective dose to adult patients from 338 radiopharmaceuticals estimated using ICRP biokinetic data, ICRP/ICRU computational reference phantoms and ICRP 2007 tissue weighting factors *EJNMMI Phys.* 2014 1:9.
- Andersson, M. Erratum to: Effective dose to adult patients from 338 radiopharmaceuticals estimated using ICRP biokinetic data, ICRP/ICRU computational reference phantoms and ICRP 2007 tissue weighting factors. *EJNMMI Phys.* 2015 2:22.
- Barrett, P.H., Bell, B.M., Cobelli, C., Golde, H., Schumitzky, A., Vicini, P. SAAM II: Simulation, analysis, and modeling software for tracer and pharmacokinetic studies. *Metabolism* 1998 47(4):484–492.
- Beamish, M. R., Brown, E. B. The metabolism of transferrin bound ^{111}In and ^{59}Fe in rat. *Blood* 1974 43:693-701.
- Bolch, W. E., Eckerman, K. F., Squoros, G., Thomas, S. R. MIRD pamphlet No. 21: a generalized schema for radiopharmaceutical dosimetry—standardization of nomenclature. *J. Nucl. Med.* 2009 50:477–484.
- Castronovo, FP., Wagner, HN. Factors affecting the toxicity of the element indium. *Br. J. Exp. Pathol.* 1971 52(5):543-59.
- Castronovo, FP., Wagner, HN. Comparative toxicity and pharmacodynamics of ionic indium chloride and hydrated indium oxide. *J. Nucl. Med.* 1973 14(9):677-82.
- Cloutier, R.J., Smith S.A., Watson E.E., Snyder W.S., Warner, G.G. Dose to the fetus from radionuclides in the bladder. *Health Phys.* 1973 25:147-161.
- Covens, P., Berus, D., Caveliers, V., Struelens, L., Vanhavere, F., Verellen, D. Skin dose rate conversion factors after contamination with radiopharmaceuticals: influence of contamination area, epidermal thickness and percutaneous absorption. *J. Radiol. Prot.* 2013 33(2):381-393.
- Cristy, M., Eckerman, K. Specific absorbed fractions of energy at various ages from internal photons sources. ORNL/TM-8381 V1-V7. Oak Ridge National Laboratory 1987.
- Finsterer, U., Prucksunand, P., Brechtelsbauer, H. Critical evaluation of methods for determination of blood volume in the dog. *Pflügers Arch* 1973 341:63–72.
- Giussani, A., Uusijärvi, H. Biokinetic models for radiopharmaceuticals. In: Cantone MC, Hoeschen C (eds), Radiation physics in nuclear medicine. Springer, Berlin 2011 233-255.
- Glaubitt, D.M., Schlüter, I.H., Haberland, K.U. Bone marrow imaging using ^{111}In -citrate: ^{111}In -kinetics in the pelvic region. *J. Nucl. Med.* 1975 16(8):769-74.

- Goodwin, D.A., Goode, R., Brown, L., Imbornone, C.J. ¹¹¹In-labeled transferrin for the detection of tumors. *Radiology* 1971 100(1):175-9.
- Goris, M. *Nuclear Medicine Applications and their Mathematical Basics*. World Scientific, Danvers MA, USA 2011.
- Gustafsson, J., Brolin, G., Cox, M., Ljungberg, M., Johansson, L., Gleisner, K. S. Uncertainty propagation for SPECT/CT-based renal dosimetry in ¹⁷⁷Lu peptide receptor radionuclide therapy. *Phys. Med. Biol.*, 2015 Nov 7;60(21):8329-46. doi: 10.1088/0031-9155/60/21/8329. Epub 2015 Oct 12.
- Hadid, L., Gardumi, A., Desbree, A. Evaluation of absorbed and effective doses to patients from radiopharmaceuticals using the ICRP 110 Reference computational phantoms and ICRP 103 formulation. *Radiat. Prot. Dosim.* 2013 156:141–159.
- Harrison, J.D., Balonov, M., Martin, C. J., Ortiz Lopez, P., Menzel, H.-G., Simmonds, J. R., Smith-Bindman, R., Wakeford, R. Use of effective dose. *Ann. ICRP* 2016 45(1S):215-224.
- Hosain, F., McIntyre, P. A., Poulouse, K., Stern, H.S., Wagner, H.N. Binding of trace amounts of ionic indium-113m to plasma transferrin. *Clinica Chimica Acta* 1969 24(1):69-75.
- Humm, J.L., Howell, R.W., Rao, D.V. Dosimetry of Auger-electron-emitting radionuclides: report no. 3 of AAPM Nuclear Medicine Task Group No. 6. *Med. Phys.* 1994 21:1901–1915.
- ICRP. Report of the task group on reference man. ICRP Publication 23. Pergamon 1975.
- ICRP. Recommendations of the International Commission on Radiological. ICRP Publication 26. Oxford. Pergamon Press 1977.
- ICRP. Statement from the 1978 Stockholm meeting of the ICRP. ICRP Publication 28. Oxford. Pergamon Press 1978.
- ICRP. Limits for intakes of radionuclides by workers. ICRP Publication 30 (Part 1). *Ann. ICRP* 1979 2(3-4).
- ICRP. Radiation Dose to Patients from Radiopharmaceuticals. ICRP Publication 53. *Ann. ICRP*, 1987 18(1-4).
- ICRP. 1990 Recommendations of the International commission on radiological protection. ICRP Publication 60 *Ann. ICRP* 1991 21(1-3).
- ICRP. Radiation dose to patients from radiopharmaceuticals (Addendum to ICRP Publication 53). ICRP Publication 80. *Ann. ICRP* 1998 28(3).
- ICRP. Basic anatomical and physiological data for use in radiological protection. ICRP Publication 89. Reference Values. *Ann. ICRP* 2002 32(3-4).
- ICRP. Human alimentary tract model for radiological protection. ICRP Publication 100. *Ann. ICRP* 2006 36(1-2).
- ICRP. The 2007 recommendations of the International commission on radiological protection. ICRP Publication 103. *Ann. ICRP* 2007 37 (2-4).
- ICRP. Radiation dose to patients from radiopharmaceuticals –addendum 3 to ICRP Publication 53. ICRP Publication 106. *Ann. ICRP* 2008 38(1-2).
- ICRP. Nuclear decay data for dosimetric calculations. ICRP Publication 107. *Ann. ICRP* 2008b 38(3).

- ICRP. Adult reference computational phantoms. ICRP Publication 110. Ann. ICRP 2009 39(2).
- ICRP. Conversion coefficients for radiological protection quantities for external radiation exposures. ICRP Publication 116. Ann. ICRP 2010 40(2-5).
- ICRP. ICRP Statement on tissue reactions / early and late effects of radiation in normal tissues and organs – threshold doses for tissue reactions in a radiation protection context. ICRP Publication 118. Ann. ICRP 2012 41(1/2).
- ICRP. Radiation dose to patients from radiopharmaceuticals: a compendium of current information related to frequently used substances. ICRP Publication 128. Ann. ICRP 2015 44(2S).
- ICRP. Occupational intakes of radionuclides: Part 1. ICRP Publication 130. Ann. ICRP 2015b 44(2).
- ICRP. The ICRP computational framework for internal dose assessment for reference adults: specific absorbed fractions. ICRP Publication 133. Ann. ICRP 2016 45(2).
- ICRU. Fundamental quantities and units for ionizing radiation(revised) ICRU report no.85 Journal of the ICRU 11. 2011..
- Jeffcoat, M.K., McNeil, B. J., Davis, M.A. Indium and iron as tracers for erythroid precursors. J. Nucl. Med. 1978 19(5):496-500.
- Johansson, L. Patient irradiation in diagnostic nuclear medicine: Assessment of absorbed dose and effective dose equivalent dosimetry [doctoral thesis]. Gothenburg, Sweden: Gothenburg University 1985.
- Joshi, A.D., Pontecorvo, M.J., Adler, L., Stabin, M.G., Skovronsky, D.M., Carpenter, A.P., Mintun, M.A., Florbetapir f study investigators. Radiation dosimetry of florbetapir ¹⁸F. EJNMMI Res. 2014 4(1):4.
- Jönsson, B.A. Biokinetics and localization of some In-111-radiopharmaceuticals in rats at the macroscopic and microscopic level: an approach towards small scale dosimetry [doctoral thesis]. Lund, Sweden: Lund University 1991.
- Kim, H., Yeom, Y.S., Nguyen, T., Choi, C., Han, M., Lee, J.K., Kim, C., Zankl, M., Petoussi-Hens, N., Bolch, W., Lee, C., Qiu, R., Eckerman, K. Chung. B. Inclusion of thin target and source regions in alimentary and respiratory tract systems of mesh-type ICRP adult reference phantoms Phys. Med. Biol. at press: <https://doi.org/10.1088/1361-6560/aa5b72> 2017.
- Koeppel, R. Principles of compartmental analysis and physiologic modeling. In Robert E Henkin MD, FACNP (ed) Nuclear medicine, vol I. Mosby, St Louis. 1996 292-315.
- Koole, M. Lewis, D.M., Buckley, C., Nelissen, N., Vandenbulcke, M., Brooks, D.J., Vandenberghe, R., Van Laere, K. Whole-body biodistribution and radiation dosimetry of ¹⁸F-GE067: a radioligand for in vivo brain amyloid imaging. J. Nucl. Med. 2009 50(5):818–822.
- Leggett, R.W., Eckerman, K.F., Williams, L.R. An Elementary method for implementing complex biokinetic models Health Phys. 1993 64(3):260-271.
- Leggett, R.W., Williams, L.R. A proposed blood circulation model for Reference Man. Health Phys. 1995 69:187-201.
- Leggett, R.W., Giussani, A. A biokinetic model for systemic technetium in adult humans. J. Radiol. Prot. 2015 35:297–315.

- Lilien, D.L., Berger, H.G., Anderson, D.P., Bennett, L.R. ¹¹¹In-chloride: a new agent for bone marrow imaging. *J. Nucl. Med.* 1973 14(3):184-6.
- Lin, K.J., Hsu, W.C., Hsiao, I.T., Wey, S.P., Jin, L.W., Skovronsky, D., Wai, Y.Y., Chang, H.P., Lo, C.W., Yao, C.H., Yen, T.C., Kung, M.P. Whole-body biodistribution and brain PET imaging with [18F] AV-45, a novel amyloid imaging agent—a pilot study. *Nucl. Med. Biol.* 2010 37(4):497–508.
- Loevinger, R., Berman, M. A schema for absorbed-dose calculations for biologically-distributed radionuclides. MIRD Pamphlet No. 1. New York, NY: Society of Nuclear Medicine 1968
- Mattsson, S., Patient dosimetry in nuclear medicine. *Rad. Prot. Dosim.* 2015 165(1-4):416-423.
- McIntyre, P.A., Larson, S.M., Eikman, E.A., Colman, M., Scheffel, U., Hodgkinson, B.A. Comparison of the metabolism of iron-labeled transferrin (Fe-TF) and indium-labeled transferrin (In-TF) by the erythropoietic marrow. *J. Nucl. Med.* 1974 15(10):856-62.
- Nakai, T., Okuyama, C., Kubota, T., Kobayashi, K., Tsubokura, T., Ushijima, Y., Nishimura, T. Pattern of ¹¹¹In-chloride bone marrow scintigraphy in myelodysplastic syndrome; comparison with clinical characteristics. *Ann. Nucl. Med.* 2004 18(8):675-80.
- Norrgrén, K., Leide Svegborn, S., Areberg, J., Mattsson, S. Accuracy of the quantification of organ activity from planar gamma camera images. *Cancer Biother Radiopharm* 2003 18:125-31.
- Noßke, D., Mattsson, S., Johansson, L. Dosimetry in nuclear medicine diagnosis and therapy. In: *Medical Radiological Physics* (Ed. by A Kaul), Landolt-Börnstein, New Series VIII/7A, Springer-Verlag, Berlin Heidelberg 2012 4:1-62.
- O’Keefe, G.J., Saunder, T.H., Ng, S., Ackerman, U., Tochon-Danguy, H.J., Chan, J.G., Gong, S., Dyrks, T., Lindemann, S., Holl, G., Dinkelborg, L., Villemagne, V., Rowe, C. Radiation dosimetry of beta-amyloid tracers ¹¹C-PiB and ¹⁸F-BAY94-9172. *J. Nucl. Med.* 2010 50(2):309–315.
- Pawel, D. J., Leggett, R.W., Eckerman K.F., Nelson C.B. Uncertainties in cancer risk coefficients for environmental exposure to radionuclides: an uncertainty analysis for risk coefficients reported in Federal Guidance Report No. 13. Oak Ridge National Laboratory. ORNL/TM-2006/583 2007.
- Roedler, H.D. Accuracy of internal dose calculations with special consideration of radiopharmaceutical biokinetics. In: *Third International radiopharmaceutical dosimetry symposium* (Proc. Conf. Oak Ridge, TN, 1980), HSS Publication (FDA 81-8166). Rockville, MD: Department of health and human welfare, Bureau of radiological health 1980.
- Sayle, B.A., Helmer, R.E. 3rd., Birdsong, B.A., Balachandran, S., Gardner, F.H. Bone-marrow imaging with indium-111 chloride in aplastic anemia and myelofibrosis: concise communication. *J. Nucl. Med.* 1982 23(2):121-125.
- Scheinin N, Tolvanen T, Wilson I, Arponen, E.M., Nägren, K.A., Rinne, J.O. Biodistribution and radiation dosimetry of the amyloid imaging agent ¹¹C-PIB in humans. *J. Nucl. Med.* 2007 48:128–133.
- Segars, W.P., Sturgeon, G., Mendonca, S., Grimes, J., Tsui, B. 4D XCAT phantom for multimodality imaging research. *Med. Phys.* 2010 37:4902–4915.

- Simonsen, J.A., Braad, P.E., Veje, A., Gerke, O., Schaffalitzky De Muckadell, O.B., Hoiland-Carlsen P.F. (111)Indium-transferrin for localization and quantification of gastrointestinal protein loss. *Scand. J. Gastroenterol.* 2009 44:1191-1197.
- Smith, G.A., Thomas, R.G., Scott, J.K. The metabolism of indium after administration of a single dose to the rat by intratracheal, subcutaneous, intramuscular and oral injection. *Health Phys.* 1960 4:101-108.
- Snyder, W.S., Ford, M.R., Warner, G.G., Watson, S.B. A tabulation of dose equivalent per microcurie-day for source and target organs for an adult for various radionuclides. US energy research and development administration report ORNL-5000, Springfield, VA, National Technical Information Service 1974.
- Snyder, W.S., Ford, M.R., Warner, G.G., Watson, S.B. "S" absorbed dose per unit cumulated activity for selected radionuclides and organs, MIRD Pamphlet No. 11. New York Society of Nuclear Medicine 1975.
- Snyder, W.S., Ford, M.R., Warner, G.G., Watson, S.B. Estimates of specific absorbed fractions for photon sources uniformly distributed in various organs of a heterogeneous phantom. MIRD Pamphlet No. 5, revised. New York Society of Nuclear Medicine 1978.
- Stabin, M. G., Sparks, R. B. and Crowe, E. OLINDA/EXM: the second-generation personal computer software for internal dose assessment in nuclear medicine. *J. Nucl. Med.* 2005 46:1023–1027.
- Stabin, M.G. Fundamentals of nuclear medicine dosimetry. Springer, New York, NY, February 2008.
- Stabin, M.G. Uncertainties in internal dose calculations for radiopharmaceuticals. *J. Nucl. Med.* 2008b 49:853–860.
- Svegborn S.L., Radiation exposure of the patient in diagnostic nuclear medicine. Experimental studies of the biokinetics of ¹¹¹In-DTPA-D-Phe1-octreotide, ^{99m}Tc-MIBI, ¹⁴C-triolein and ¹⁴C-urea and development of dosimetric models [doctoral thesis]. Lund, Sweden: Lund University 1999.
- Thomas, S. R., Stabin, M. G., Chen, C. T., Samaratunga, R. C. MIRD Pamphlet No. 14: a dynamic urinary bladder model for radiation dose calculations *J. Nucl. Med.* 1992 33:783–802.
- Thomas, S. R., Stabin, M. G., Chen, C. T., Samaratunga, R. C. MIRD Pamphlet No. 14 revised: a dynamic urinary bladder model for radiation dose calculations *J. Nucl. Med.* 1999 40:102S–23S.
- Xu, G., Eckerman, K.F. eds. Handbook of anatomical models for radiation. Dosimetry. Boca Raton, FL: CRC Press 2009.
- Yamauchi, H., Takahashi, K., Yamamura, Y., Fowler, B.A. Metabolism of subcutaneous administered indium arsenide in the hamster. *Toxicol. Appl. Pharmacol.* 1992 116:66-67.
- Zankl, M., Wittmann, A. The adult male voxel model "Golem" segmented from whole-body CT patient data. *Radiat. Environ. Biophys.* 2001 40(2):153–162.
- Zankl, M., Becker, J., Fill, U., Petoussi-Henss, N., Eckerman, K. GSF male and female adult voxel models representing ICRP Reference Man—the present status. In: Proceedings of the Monte

Carlo Method Versatility Unbounded Dynamic Computing World: April 17–21, 2005.
Chattanooga TN: Chattanooga TN 2005.

Zankl, M., Schlattl, H., Petoussi-Henss, N., Hoeschen, C. Electron specific absorbed fractions for the adult male and female ICRP/ICRU reference computational phantoms. *Phys. Med. Biol.* 2012 57:4501–4526.

Zanzonico, P.B. Internal radionuclide radiation dosimetry: a review of basic concepts and recent developments. *J. Nucl. Med.* 2000 41:297–308.



Internal dosimetry of radiopharmaceuticals in diagnostic nuclear medicine is based on biokinetic and anatomical models. The biokinetic model describes the uptake and retention of the radionuclide through the human body and where the nuclide decays. The anatomical models are mathematical models and are used to estimate the energy absorbed in the body from each decay. This means that the regions defining the biokinetic models also have to be defined in the mathematical anatomic models. A new biokinetic model is created and older models are modified to fit the new adult anatomic models presented by the ICRP and ICRU. New tools are developed to facilitate the use of the new voxel based anatomic models to perform revised adsorbed dose and effective dose estimations. This book is the doctoral thesis of Martin Andersson and discusses the implementation of new voxel based mathematical models into diagnostic nuclear medicine. When not working with internal dosimetry Martin likes long walks by the beach and fine dining.



LUND UNIVERSITY
Faculty of Medicine

Department of Translational Medicine
Medical Radiation Physics Malmö

Lund University, Faculty of Medicine
Doctoral Dissertation Series 2017:57
ISBN 978-91-7619-437-9
ISSN 1652-8220

